

# Rhein Alleviates Cisplatin-Induced Acute Kidney Injury via Downregulation of NOX4-COX2/PGFS Signaling Pathway

Xi Yuan <sup>1,2</sup>, Luosha Long <sup>1,2</sup>, Minghui Wang <sup>1,2</sup>, Wenhao Chen <sup>1,2</sup>, Baien Liang <sup>2,3</sup>, Long Xu <sup>1,2</sup>, Weidong Wang <sup>2,3</sup>, Chunling Li <sup>1,2</sup>

<sup>1</sup>Department of Physiology, Zhongshan School of Medicine, Sun Yat-Sen University, Guangzhou, People's Republic of China; <sup>2</sup>Institute of Hypertension, Zhongshan School of Medicine, Sun Yat-sen University, Guangzhou, People's Republic of China; <sup>3</sup>Department of Pathophysiology, Zhongshan School of Medicine, Sun Yat-Sen University, Guangzhou, People's Republic of China

Correspondence: Chunling Li, Department of Physiology, Zhongshan School of Medicine, Sun Yat-sen University, 74# Zhongshan Er Road, Guangzhou, 510080, People's Republic of China, Tel/Fax +86-20-87334840, Email lichl3@mail.sysu.edu.cn

**Purpose:** Cisplatin (cis-diamminedichloroplatinum II, CDDP), a widely used chemotherapeutic agent, is clinically limited by nephrotoxicity. Rhein, an anthraquinone from *Radix Rhein Et Rhizome*, shows nephroprotective potential. This study investigated Rhein's protective effects and mechanisms in CDDP-induced acute kidney injury (AKI).

**Methods:** Network pharmacology identified active components and target genes of *Radix Rhein Et Rhizome*. Bioinformatics analysis screened differentially expressed genes and conducted functional enrichment (GO/HALLMARK). Molecular docking and molecular dynamic (MD) simulations confirmed Rhein's binding to target proteins. CDDP-induced AKI mouse models and human proximal tubular epithelial cells (HK2) injury models were established to reveal Rhein's nephroprotective mechanisms. Lewis lung carcinoma (LLC) tumor-bearing mice and human A549 lung cancer cells further validated Rhein's compatibility with CDDP antitumor efficacy.

**Results:** Network pharmacology revealed 12 bioactive components and 420 potential targets of *Radix Rhein Et Rhizome*, with Rhein as the core component interacting with 50 cross-validated targets. Protein-protein interaction (PPI) network analysis prioritized 16 hub genes functionally enriched in oxidative stress (GO) and inflammatory/apoptotic pathways (HALLMARK). Molecular docking and MD simulations demonstrated Rhein's robust binding stability with NOX4, COX2, and PGFS, indicating multi-target modulation. In vivo, Rhein attenuated CDDP-induced AKI by reducing plasma creatinine, renal KIM-1/NGAL expression, and suppressing tubular apoptosis and inflammation. In vitro, Rhein mitigated CDDP-triggered HK2 cell injury through reducing ROS levels and inhibiting the NOX4-NFκB-COX2/PGFS axis. Notably, Rhein preserved CDDP's tumor-suppressive effects in both LLC-bearing mice and A549 cells.

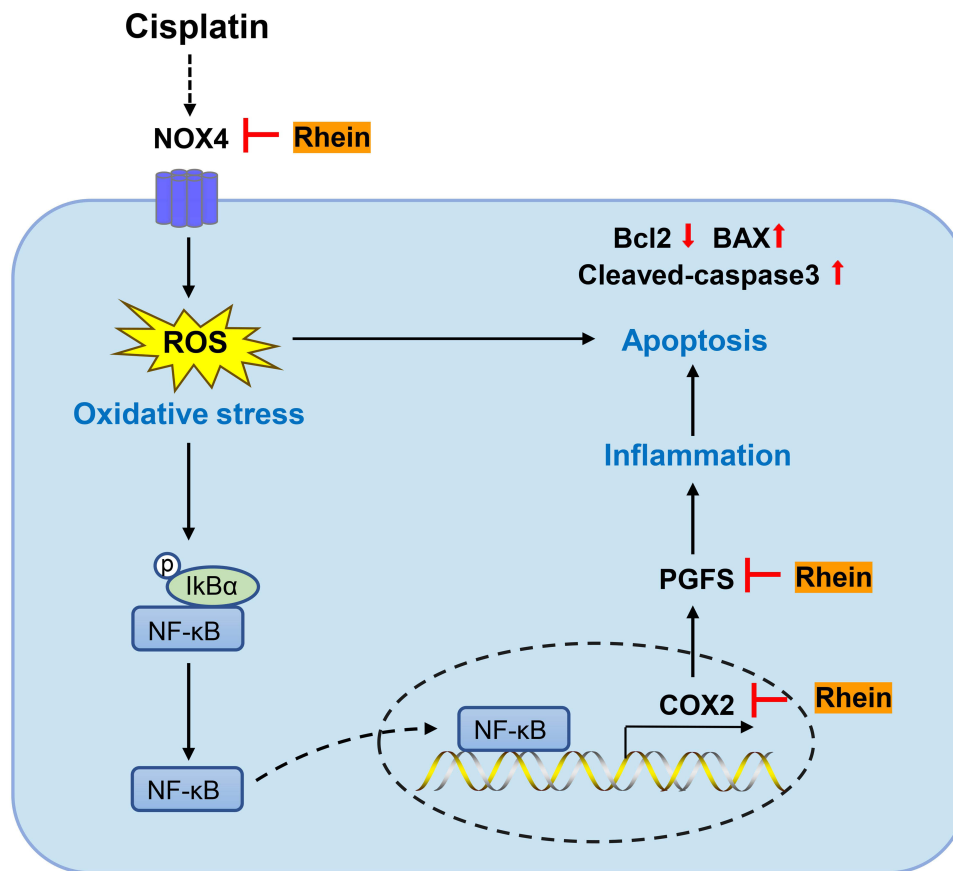
**Conclusion:** Rhein protects against CDDP-induced AKI by inhibiting oxidative stress and inflammation through targeting the NOX4-NFκB-COX2/PGFS pathway, without compromising CDDP's antitumor activity. These findings highlight Rhein as a promising adjunctive therapy for CDDP-associated nephrotoxicity.

**Keywords:** rhein, cisplatin, acute kidney injury, inflammation, oxidative stress

## Introduction

Acute kidney injury (AKI), a global health problem with the increase of morbidity and mortality in each year, is characterized by a decline in renal filtration function and a rapid accumulation of metabolic waste products.<sup>1</sup> Clinically, the most common causes of AKI include nephrotoxins, ischemia-reperfusion injury and sepsis. Drug-induced nephrotoxicity accounts for 6% of community-acquired AKI and 20% of hospital-acquired AKI.<sup>2</sup> Cisplatin (cis-diamminedichloroplatinum II, CDDP) is one of the most widely used chemotherapeutics, however, its clinical application is limited by the dose-related nephrotoxicity.<sup>3</sup> It is eliminated from the kidney and accumulates in renal tubular cells, resulting in tubular cell injury and death.<sup>4</sup> Approximately 30% of patients undergoing CDDP treatment develop renal dysfunction, with AKI as the most common manifestation.<sup>5</sup> Further, the pathophysiology of CDDP-induced AKI mainly

## Graphical Abstract



involves oxidative stress, apoptosis, inflammation and abnormal autophagy.<sup>3</sup> The current therapies for CDDP-induced AKI, such as hydration and forced diuresis, are interventions for symptomatic but not disease courses based on pathological mechanisms. Moreover, these therapies are associated with a series of side effects.<sup>6</sup> Therefore, there is an urgent need to discover safe and effective drugs for adjuvant treatment.

Reactive oxygen species (ROS) are natural byproducts of cellular metabolism that serve pivotal roles in various physiological functions.<sup>7</sup> Elevated levels of ROS can induce oxidative stress, a condition observed in kidney injury triggered by chemotherapy, such as CDDP.<sup>8</sup> Increased ROS may derive from the pathways associated with NADPH oxidases (NOXs),<sup>9</sup> nitric oxide synthase,<sup>10</sup> and inflammation.<sup>11</sup> Escalated oxidative stress can trigger various redox signaling responses, including the activation of nuclear factor-kappa-B (NF-κB), nuclear factor erythroid 2-related factor (Nrf2) and mitogen-activated protein kinases (MAPK), which subsequently govern gene expression, inflammation, stress-related immune reactions, and repair mechanisms.<sup>12</sup>

Recent *in vitro* and *in vivo* studies have shown that many natural products from traditional Chinese medicine (TCM) have specific antioxidant, anti-inflammatory and anti-apoptotic properties that can modulate pathways associated with CDDP-induced kidney injury.<sup>13</sup> From a taxonomical perspective, currently reported natural compounds with protective effects against CDDP nephrotoxicity include flavonoids, saponins, alkaloids, polysaccharides and phenylpropanoids, etc.<sup>14</sup> However, the components of TCM are complex, and the mechanism for treatment of kidney diseases is imprecise and confounding.

Rhein, an anthraquinone compound isolated from traditional Chinese medicine *Radix Rhein Et Rhizome/Rhubarb*, is known for its multiple pharmacological activities, including anti-inflammatory, antioxidant, antitumor and apoptotic modulation properties.<sup>15,16</sup> Extensive studies have demonstrated that Rhein exerts renoprotective effects on some kidney

diseases, such as renal fibrosis, 5/6 nephrectomied-induced chronic kidney disease, and uric acid nephropathy.<sup>17–19</sup> Rhein has also been reported to significantly improve adriamycin-induced renal function decline, by regulating the activities of NF- $\kappa$ B and caspase-3 at the early stage of glomerulosclerosis in rats.<sup>20</sup> In the recent studies, network pharmacology combined with molecular docking were employed to investigate the potential mechanism of *Rhubarb* in diabetic nephropathy.<sup>21</sup> However, whether Rhein exerts a protection role on CDDP-induced AKI and its potential therapeutic targets are still unknown.

The current study aims to examine the mechanism by which Rhein prevents CDDP-induced AKI from the perspective of network pharmacology and bioinformatics, together with validation from in vivo and in vitro experiments. We provide evidence that Rhein alleviates CDDP-induced oxidative and inflammatory stress in the kidney likely through modulating NOX4-NF- $\kappa$ B-COX2/PGFS signaling.

## Materials and Methods

The flowchart of this study is shown in [Supplementary Figure S1](#).

### Screening for the Potential Target Genes of Radix Rhei Et Rhizome

The target proteins of *Radix Rhei Et Rhizome* were collected from the Traditional Chinese Medicine Systems Pharmacology Database and Analysis Platform (TCMSP, <https://old.tcm-sp-e.com/tcm-sp.php>), High-throughput experiment- and reference-guided database of traditional Chinese medicine (HERB, <http://herb.ac.cn/>), Similarity ensemble approach database (SEA, <https://sea.bkslab.org/>), a comprehensive database of Traditional Chinese Medicine on Immuno-Oncology (TCMIO, <http://tcmio.xielab.net/>) and Swiss Target Prediction database (SwissTarget, <http://www.swisstargetprediction.ch/>). After merging the results of these databases and removing duplicate targets, target proteins were transformed into standard gene names by the UniProt database (<https://www.uniprot.org/>).

### Identification of Differentially Expressed Genes (DEGs) in CDDP-Induced AKI Model

The target genes implicated in CDDP-induced AKI were obtained from the NCBI Gene Expression Omnibus database (GEO, <https://www.ncbi.nlm.nih.gov/geo/>). Gene expression profiles of GSE145085 dataset based on the GPL18573 Illumina NextSeq 500 platform (*Homo sapiens*), GSE98602 dataset based on GPL17303 Ion Torrent Proton (*Homo sapiens*), GSE85957 dataset based on the Affymetrix Rat Genome 230 2.0 Array, GSE37133 dataset based on the ABI Rat Genome Survey Microarray, GSE147256 and GSE153625 dataset based on the Illumina HiSeq 4000 (*Mus musculus*). The “edgeR”<sup>22</sup> package was used to identify DEGs between the drug intervention and normal samples. Adjusted *P*-value < 0.05 and  $|\log_2$  (fold change)  $\geq 1$  were chosen as the cut-off threshold.

### Screening Common Genes of Rhein-Targeted Genes and DEGs From CDDP-Induced AKI Model

The common targets between Rhein and CDDP-induced AKI were intersected using the VENNY 2.1 online platform (<https://bioinfogp.cnb.csic.es/tools/venny/index.html>, accessed on 8 Mar 2024).

### Protein-Protein Interaction (PPI) Network Construction

The PPI network of common targets was constructed using the STRING database (<https://cn.string-db.org/>). The organism was set to *Homo sapiens*; confidence scores were larger than 0.5, and the other variables remained as the default. Thereafter, the Protein-Protein Interaction (PPI) network was exported in TSV format and analyzed using Cytoscape\_v3.9.1 software (<https://cytoscape.org/>). PPI networks were formed with nodes (indicating a target protein) and edges. The degree indicates the number of nodes directly connected to a node. Core targets were identified using the Cytoscape plugin (Network Analysis). Here, the top 12 upregulated proteins were selected as core targets based on their degree ranking.

## Gene Function and Pathway Enrichment Analysis

Gene Ontology (GO) and HALLMARK enrichment analysis were conducted on the DEGs by using the “clusterProfiler” R package.<sup>23</sup> False discovery rate < 0.05 was considered statistically significant.

## Molecular Docking

KDR (PDB ID: 1VR2), APP (PDB ID: 3PMR), PPARG (PDB ID: 6FZP), MMP9 (PDB ID: 1L6J), PTGS2 (PDB ID: 5IKT), EGFR (PDB ID: 3W2S), CYP1B1 (PDB ID: 3PM0), PGFS (PDB ID: 3R8G), MET (PDB ID: 3DKC), NOX4 (UniProt ID: E9PR43), PIK3R1 (PDB ID: 7PG5), and AHR (PDB ID: 5L9V) crystal structures were obtained from Protein Data Bank (PDB) database (<https://www.rcsb.org/>) or UniProt database. The chemical structures of the Rhein were achieved from the NCBI PubChem database (<https://pubchem.ncbi.nlm.nih.gov/>). Water molecules and unwanted ligands from the selected target proteins were removed using PyMOL™ 2.5.1. The receptor proteins were modified and small molecular ligand was performed using Autodock vina 1.2.4. Affinity scores were used to evaluate the binding potential between the top 12 core target proteins and Rhein. The SYBYL SYBYL-X 2.0 software (Tripos, St. Louis, MO) was used to assign the standard Assisted Model Building with Energy Refinement (AMBER) atomic partial charges on the receptor proteins and the GasteigerHückel atomic partial charges on the ligand candidates to be docked. After these procedures, the docking was carried out in SYBYL software under default setting, and the figures were obtained by utilizing PyMol (<http://www.pymol.org>).

## Molecular Dynamic Simulation

Molecular dynamic (MD) simulations were conducted using Gromacs 2020.6 software. The force field parameters for Rhein were derived utilizing the CHARMM General Force Field (CGenFF) 36 and the CHARMM-GUI web interface 67 (<https://app.cgenff.com/>). The protein crystal structures of NOX4, COX2, and PGFS were sourced from either the PDB database or UniProt database. The subsequent procedures included establishing periodic boundaries for the MD simulations and creating a cubic box that extended 1.0 nm from the protein’s surface. The system was then hydrated using the TIP3P water model. To balance the charges in the system, Na and Cl ions were introduced to neutralize the protein’s charge. The equilibrated systems underwent unrestrained production MD simulations for 100 ns while maintaining a target pressure of 1 bar and a temperature of 300 K. The MD trajectory was analyzed using GROMACS utilities to extract root-mean-square fluctuation (RMSF), root-mean-square deviation (RMSD), radius of gyration (Rg), and solvent-accessible surface area (SASA). Finally, DuIvyTools 0.5.0 was employed to visualize the results.

## Chemicals and Reagents

Cisplatin (CDDP, P4394, purity≥98%) were purchased from Sigma-Aldrich (St. Louis, MO, USA). Rhein for animal experiments (F21820-5g, purity≥98%) was purchased from Shanghai Mairuier Chemical Technology Co., Ltd (Shanghai, China). Rhein for cell experiments (10 mM/1 mL, T2997, purity≥98%) was purchased from TargetMol (Boston, USA). Antibodies against COX2 (sc-376861), p65 (sc-8008), p-p65 (sc-135769) were obtained from Santa Cruz Biotechnology (Santa Cruz, CA, USA). Antibodies against BAX (#2772S) and cleaved-caspase-3 (#8664S) were purchased from Cell Signaling Technology (CST, USA). Antibodies against Bcl2 (68,103-1-Ig), cleaved-caspase-3 (68,773-1-Ig), p65 (80,979-1-RR), p-p65 (82,335-1-RR), NOX4 (14,347-1-AP), PGFS (AKR1C3, 11,194-1-AP) and β-actin (81115-1-RR) were purchased from Proteintech Group (Wuhan, China). Antibodies against p-IkBα (BS-18128) and IkBα (BS-1287) were purchased from Bioss (Bioss, Beijing, China). The information of antibodies is presented in [Table S1](#). One-step Terminal deoxynucleotidyl transferase dUTP nick end labeling (TUNEL) In Situ Apoptosis Kit (Elab Fluor® 594, E-CK-A322) was purchased from Elabscience Biotechnology (Elabscience, Wuhan, Hubei, China). Reactive Oxygen Species Assay Kit (S0033S) and Cell Counting Kit-8 (C0038) were purchased from Byotime Biotechnology (Shanghai, China).

## Animal Models and Treatment

Male C57BL/6 mice (8 weeks old) were provided by the Medical Experimental Animal Center of Guangdong Province (Guangdong, China), production license number: SCXK(Yue)2022–0002. Animals were housed under a 12-h light/dark

cycle at 18–22°C room temperature with food and water available ad libitum. All animal procedures were conducted following the Guidelines for the Ethical Review of Laboratory Animal Welfare (China, 2018) and approved by the Institutional Animal Care and Use Committee (IACUC) of Sun Yat-sen University (Approval No. 2023001813). Male C57BL/6 mice were acclimatized for one week before the study. Randomization of mice into groups was done using the random number table method, and all operators were blinded to the group assignments. CDDP was dissolved in preheated saline solution (55°C), while Rhein was suspended in 1.25% sodium carboxymethylcellulose (CMC-Na). The doses of both drugs were determined based on preliminary experiments and published studies.<sup>24,25</sup>

### Protocol I

To investigate the protective effects of Rhein on CDDP-induced AKI, mice were randomly divided into four groups (n=5):

Control group (Group 1): Mice were received intraperitoneal saline injections and drug-free CMC-Na by gavage;

CDDP group (Group 2): Mice received a single intraperitoneal dose of CDDP (20 mg/kg, i.p) on day 1, followed by drug-free CMC-Na orally for three days;

Rhein group (Group 3): Mice received intraperitoneal saline on day 1 and orally administered Rhein (80 mg/kg/day, i.g) for three days;

CDDP+Rhein group (Group 4): Mice in this group received CDDP as in the Group 2 and Rhein as in the group 3. Three days after CDDP injection, mice were sacrificed under anaesthesia, and samples of plasma and urine were collected. Kidney tissues were harvested for further analysis.

### Protocol II

To determine whether Rhein might affect the antitumor activity of CDDP, mice were subcutaneously inoculated with CDDP-sensitive Lewis lung carcinoma (LLC, catalog no. CRL-1642, RRID:CVCL\_4358; ATCC, Manassas, VA, USA) cells ( $2 \times 10^5$ ) 14 days in advance,<sup>26</sup> and randomly divided into four groups (n=5):

Control group (Group 1): Tumor-bearing mice received intraperitoneal saline injections and drug-free CMC-Na by gavage.

CDDP group (Group 2): Tumor-bearing mice were administered with cisplatin (4 mg/kg, i.p). every other day from day 0 (cumulative dose 20 mg/kg over 8 days).

Rhein group (Group 3): Tumor-bearing mice were orally administered Rhein (80mg/kg/day) every other day from day 0 (over 8 days).

CDDP+Rhein group (Group 4): Tumor-bearing mice received CDDP as in the Group 2 and Rhein as in the group 3. On day 10 after first injection of CDDP, the tumors were removed and weighed, and the tumor size was measured.

## Cell Culture and Treatment

Human proximal tubular epithelial cell line (HK2, catalog no. CRL-2190, RRID:CVCL\_0302) was obtained from the ATCC and were cultured in a DMEM/F12 medium at a 37°C incubator in 5% CO<sub>2</sub>. The medium was supplemented with 5% FBS, streptomycin (100 mg/mL), and penicillin (100 IU/mL).

The HK2 cells were starved of serum for 12 h before treatment during the experiments. CDDP was administered to HK2 cells at a concentration of 10 µg/mL for 24 h to establish the CDDP-induced HK2 cell injury model, the dose of CDDP was based on our preliminary experiments and the published study.<sup>27</sup> DMSO was used as a solvent control for Rhein; the same volume of DMSO was treated to cells as a control. When an appropriate confluency was reached, HK2 cells were treated with Rhein at seven concentrations of Rhein (0, 5, 10, 20, 40, 50, 80µM) for 24 h. 40 µM concentration of Rhein was selected as the final stimulation concentration for subsequent experiments.

To determine whether Rhein might affect the anti-tumor activity of CDDP in vitro, CDDP-sensitive human non-small-cell lung cancer (NSCLC) cell line A549 (catalog no. CCL-185, RRID: CVCL\_0023; ATCC, Manassas, VA, USA) was exposed to CDDP (10 µg/mL) alone or in combination with Rhein for 24h, cell viability was then measured.

## Cellular Thermal Shift Assay

Cellular thermal shift assay (CETSA) was conducted using cell lysates as previously described.<sup>28,29</sup> HK2 cells were pretreated with 40µM Rhein in an incubator containing 5% CO<sub>2</sub> at 37°C for 6h. For the temperature-dependent thermal

shift assay, the soluble protein lysate of HK2 cells was incubated with 40  $\mu$ M of Rhein at each temperature point from 37°C to 87°C for 4 minutes. The supernatant and pellet were separated from the above samples by centrifugation at 20,000g for 10 minutes. 40 $\mu$ L supernatant was mixed with 10 $\mu$ L 5 $\times$ loading buffer and then separated on a 12% SDS-PAGE for immunoblotting analysis of NOX4, COX2 and PGFS.

## Cell Viability Assay

According to the manufacturer's instructions, viability was assessed using CCK-8 kits. Cells were cultured in 96-well microplates at a density of  $5 \times 10^3$ /well in 100  $\mu$ L of medium and treated with different concentrations of Rhein for 24 h. Subsequently, 10  $\mu$ L of CCK-8 reagent was added to each well and incubated for 2 h. The absorbance of each well was measured at 450 nm.

## TUNEL Assay

The apoptosis rate of HK2 cells and renal tissues was detected by TUNEL staining. The renal tissues were embedded in paraffin and incised into thin sections (4 $\mu$ m) and HK2 cell coverslips were fixed in 4% PFA. Immunofluorescence procedures for detecting apoptotic cells were performed according to the manufacturer's instructions by using a fluorescence microscope (Leica DMi8). All sections were photographed at a magnification of 200 $\times$ .

## Histopathological Examination

Paraffin wax-embedded sections (4  $\mu$ m thick) of renal tissues from the mice were prepared. The renal tissue sections were stained with Hematoxylin and Eosin (H&E) according to the manufacturer's instructions to assess kidney injury. H&E sections were evaluated according to renal cortical vacuolization, infiltration of peritubular and proximal tubule leukocytes, and simplification of the proximal tubules. All sections were photographed at a magnification of 400 $\times$ .

## ROS Detection

To determine the intracellular ROS production, cells were incubated with 5  $\mu$ M DCFH-DA probe for 30 min at 37°C before subjected to flow cytometry analysis.

## Western Blot

Total proteins were extracted from the HK2 cells or renal cortex. The protein concentrations were detected by bicinchoninic acid (BCA) kit (23225, Thermo Scientific™, USA). Protein lysates were subjected to SDS-PAGE gels and transferred to polyvinylidene fluoride membranes. The membranes were incubated with primary antibodies against NOX4 (1:1000), COX2 (1:1000), PGFS (1:1000), BAX (1:1000), cleaved-caspase-3 (1:1000), Bcl2 (1:1000), p65 (1:2000), p-p65 (1:1000), p-IkBa (1:1000), IkBa (1:1000) and  $\beta$ -actin (1:10,000), followed by peroxidase-conjugated secondary antibodies incubation. The blots were imaged using the Tanon Chemiluminescent Imaging System (Tanon, Shanghai, China), and the band intensity was quantified by densitometric analysis using the Image J (1.41v, US National Institutes of Health, USA). The protein expression was normalized relative to  $\beta$ -actin expression.

## qPCR

Total cellular RNA from renal cortex was extracted by Trizol reagent (Invitrogen, Carlsbad, CA, USA) and reverse transcribed to cDNA by 5X Evo M-MLV RT Master Mix Kit (AG11706, ACCURATE BIOLOGY(AG)). The cDNA was subsequently used as a template for the amplification by qPCR using the SYBR Green Premix Pro Taq HS qPCR Kit (AG11740, AG) and primers. Data quantification was performed using the  $2^{-\Delta\Delta Ct}$  method. Relative expression of KIM-1 and NGAL were normalized to the GAPDH. The primers of KIM-1, NGAL and GAPDH were listed in [Table S2](#).

## Statistical Analysis

Data were shown as mean  $\pm$  standard error of the mean (SEM), and the number of repeats ( $n$ ) for each experiment was indicated in the figure legends. Statistical analysis and graphical data presentation were performed using Prism GraphPad 8.0 software. The normal distribution of the data was estimated by the Kolmogorov–Smirnov test, and statistical analyses

were performed using one-way ANOVA followed by Student-Newman-Keul's test or two-tailed Student's *t*-test. One-way repeated measures ANOVA followed by Bonferroni's post hoc test was used to assess statistical the significance of changes over time. *P*-values of 0.05 or less were considered significant.

## Results

### Screening of Active Compounds and Related Target Genes of Radix Rhein Et Rhizome

A Previous study by Zhang et al demonstrated the protective role of *Radix Rhein Et Rhizome* in kidney disease.<sup>30</sup> However, the specific protective effects of *Radix Rhein Et Rhizome* against CDDP-induced AKI and the underlying mechanisms remain incompletely understood. Here, we employed a network pharmacology approach to identify the key active components of *Radix Rhein Et Rhizome* and their associated target genes implicated in CDDP-induced AKI. Through screening for ingredients with an Oral Bioavailability (OB) value of  $\geq 30\%$  and Drug-likeness (DL) value of  $\geq 0.18$  in the TCMSP database, we identified 12 potential active compounds including *Radix Rhein Et Rhizome*, including Rhein, Eupatin, Beta-sitosterol, Daucosterol\_qt, Toralactone, Physciondiglucoside, Aloe-emodin, (-)-catechin, Emodin-1-Obeta-D-glucopyranoside, Sennoside E\_qt, Palmidin A, and Mutatochrome (Figure 1A). Further details regarding these compounds were provided in Table S3. Subsequently, we gathered target proteins associated with these 12 active compounds from the TCMSP, HERB, SEA, TCMIO and Swiss Target Prediction database. Upon consolidating and deduplicating the results of these databases, the protein targets were standardized into gene names using the UniProt database, resulting in a total of 420 target genes associated with the 12 chemical compositions (Figure 1A).

### Feature Analysis of Radix Rhein Et Rhizome-Active Compound–Target Gene Network

The target genes implicated in CDDP-induced AKI were obtained from the GEO database. The “edgeR” package was used to identify differentially expressed genes (DEGs) from AKI model of CDDP-treated human kidney organoids (GSE145085). By applying a cut-off threshold of Adjusted *P*-value  $< 0.05$  and  $|\log_2(\text{fold change})| > 1$ , a total of 6896 DEGs associated with CDDP-induced AKI were identified, with 3794 upregulated and 3102 downregulated DEGs (Figure 1B). The DEGs associated with CDDP-induced AKI and the target genes of *Radix Rhein Et Rhizome* were inputted into the online Venny 2.1 platform for intersection analysis, resulting in the identification of 136 common target genes (Figure 1C). Next, we constructed a predicted target network between *Radix Rhein Et Rhizome*, 12 active compound and 136 target genes by using Cytoscape software (Figure 1D). According to the “drug- active compound - target” network, 12 key active ingredients were ranked according to the degree values in the network (Figure 1E). The higher degree values of active ingredients, the more likely they are to have therapeutic efficacy.<sup>31</sup> Therefore, we selected Rhein (Figure 1F), an anthraquinone compound with the highest degree, for further investigation.

### Key Target Genes Regulated by Rhein in the CDDP-Induced AKI

We generated a Venn diagram to identify 50 shared genes as potential targets of Rhein in the treatment of CDDP-induced AKI, by overlaying Rhein-related target genes with DEGs from the AKI model of CDDP-treated human kidney organoids (Figure 2A). Subsequently, a predicted protein-protein interaction (PPI) network was constructed by inputting the 50 predicted targets into the STRING platform for topological analysis in Cytoscape (Figure 2B). After removing unconnected nodes, the PPI network contained 46 nodes and 206 edges (Figure 2B). Among these nodes, Kinase insert domain receptor (KDR), amyloid beta precursor protein (APP); peroxisome proliferator activated receptor gamma (PPARG); matrix metalloproteinase 9 (MMP9); prostaglandin-endoperoxide synthase 2 (PTGS2/COX2); epidermal growth factor receptor (EGFR); cytochrome P450 family 1 subfamily B member 1 (CYP1B1); aldo-keto reductase family 1 member C3 (AKR1C3/PGFS); MET proto-oncogene, receptor tyrosine kinase (MET); NADPH oxidase 4 (NOX4); phosphoinositide-3-kinase regulatory subunit 1 (PIK3R1) and aryl hydrocarbon receptor (AHR) were screened to be the 16 core node (hub genes) due to their high network degree value, betweenness centrality, and closeness centrality in the PPI regulatory network (Figure 2C).

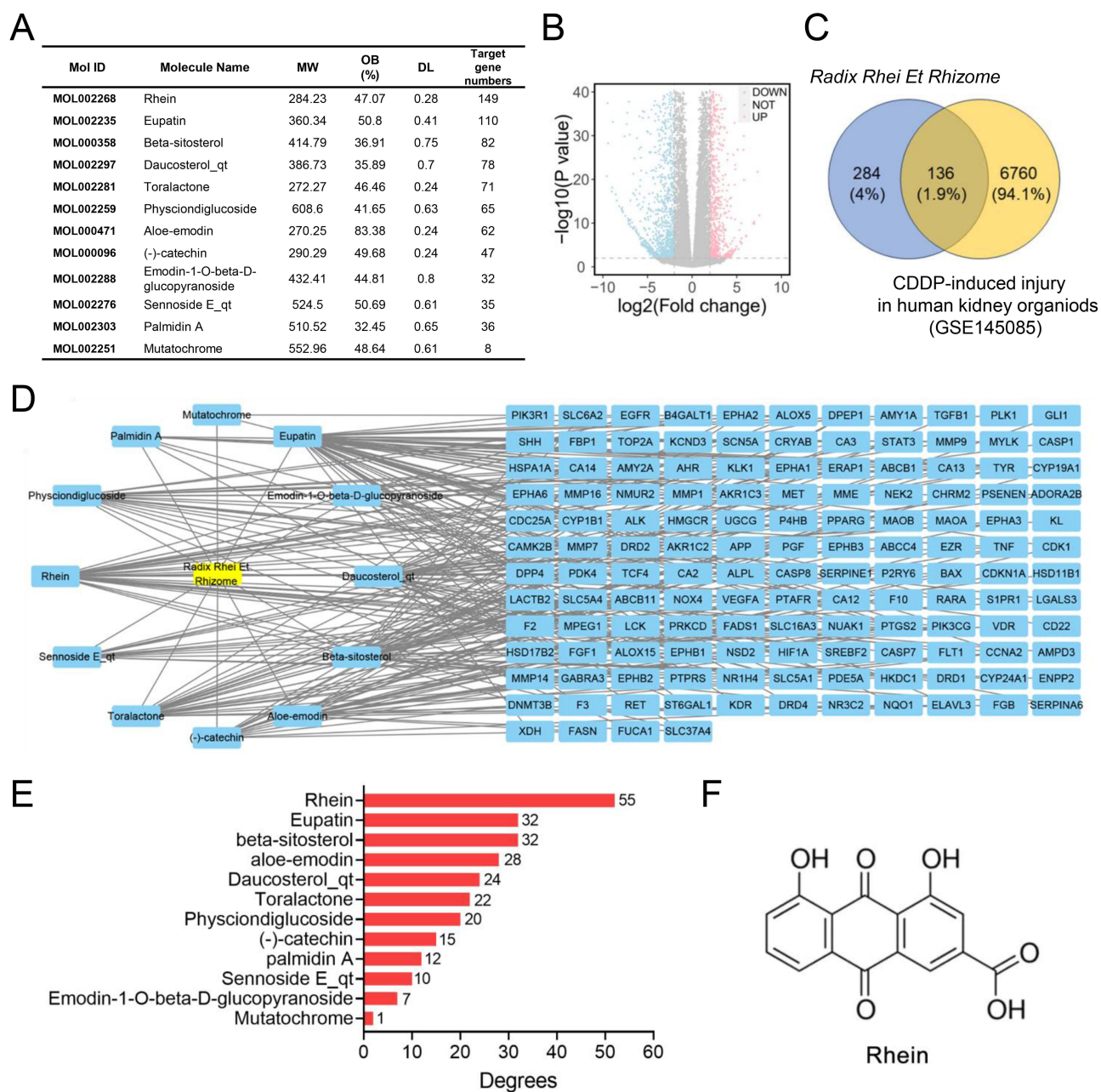


**Figure 1** Screening of active compounds and related targets of *Radix Rhei Et Rhizome*. **(A)** Main chemical constituents of *Radix Rhei Et Rhizome*. **(B)** Volcano plot of the differentially expressed genes (DEGs) analysis in AKI model of Cisplatin (CCDP)-induced human kidney organoids injury. Red or blue dots represent upregulated or downregulated genes, respectively, according to the criteria: adjusted  $P$ -value  $< 0.05$  and  $|\log_2(\text{fold change})| > 1$ . **(C)** Venn diagram depicting intersecting genes of *Radix Rhei Et Rhizome* and CCDP-induced AKI. **(D)** Component target network of 12 active ingredients of *Radix Rhei Et Rhizome* against CCDP-induced AKI, in which circular nodes represent active ingredients and rectangular nodes represent target genes. **(E)** The 12 key active ingredients ranked by degree-value. **(F)** The molecular structure of Rhein.

## Key Signaling Pathways Regulated by Rhein in CCDP-Induced AKI

Enrichment analysis of shared target genes with the clusterProfiler package based on R language and a filtering condition of  $P < 0.05$ , GO and HALLMARK pathway enrichment analyses of the 16 intersection target genes were used to determine the biological functions of kidney that were affected by Rhein. GO enrichment items were composed of biological process (BP) terms, cell composition (CC) terms, and molecular function (MF) (Figure 2D). The BP associated with CCDP-induced AKI were oxidative stress (GO: 0006979), cellular response to chemical stress (GO: 0062197), cellular response to reactive oxidative species (GO: 0034614) and response to reactive oxidative species (GO: 0000302). In the aspect of MF, there were oxidoreductase activity, acting on

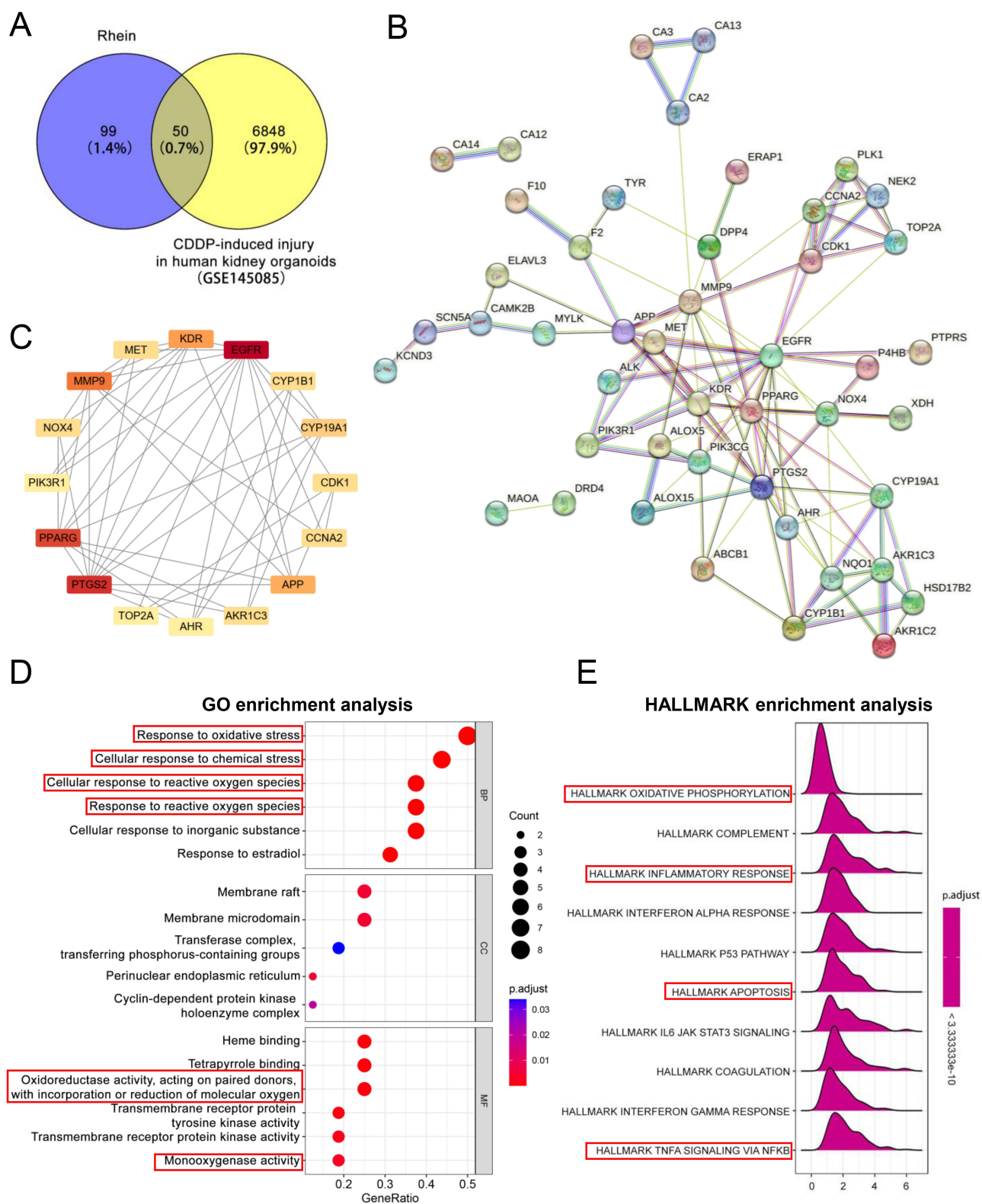


**Figure 2** Signaling pathway enrichment of Rhein-regulated core target genes in CDDP-induced AKI model. **(A)** Venn diagram showing the overlapping genes between the Rhein-targeted genes and the differentially expressed genes (DEGs) in a CDDP-induced human kidney organoid injury model. **(B)** The protein-protein interaction (PPI) network of proteins encoded by genes targeted by Rhein in CDDP-induced AKI. **(C)** The hub targets of Rhein that protect against CDDP-induced AKI were identified as 16 genes. **(D)** Gene ontology (GO) enrichment analysis of the Hub genes. "BP" stands for "biological process", "CC" stands for "cellular component" and "MF" stands for "molecular function". The size indicates the counts of enriched genes. **(E)** HALLMARK enrichment analysis of the Hub genes. The color represents the statistical significance of the term.

paired donors, with incorporation or reduction of molecular oxygen (GO: 0016705) and monooxygenase activity (GO: 0004497). The mechanism of Rhein treatment of CDDP-associated AKI may be the result of the synergistic effects of multiple pathways. These targets were subjected to MSigDB HALLMARK gene set enrichment analysis, with a total of 41 pathways, and the top 10 significantly enriched pathways were identified and selected for visualization (Figure 2E). It was shown that oxidative phosphorylation, inflammatory response, apoptosis and TNFA signaling via NF- $\kappa$ B were significantly enriched in HALLMARK Enrichment Analysis (Figure 2E).

## Molecular Docking and MD Simulation of Rhein with Key Target Proteins and Database Validation

We analyzed the expression of 16 hub genes in CDDP-induced renal organoid injury model, and found that there were 12 up-regulated genes (KDR, APP, PPARG, MMP9, PTGS2, EGFR, CYP1B1, AKR1C3, MET, NOX4, PIK3R1 and AHR) and 4 down-regulated genes (Figure 3A and B). Therefore, we conducted molecular docking between the proteins encoded by the above 12 highly expressed genes and Rhein. The binding scores were identified by Autodock vina and binding sites were visualized by PyMOL software (Figure 3C). Molecular docking results showed that Rhein docked to all 12 key target proteins with binding energies below  $-7.0$  Kcal/mol (Table S4), indicating a strong binding capacity between Rhein and these proteins. The renal pathology of CDDP-induced AKI is multifactorial, consisting of inflammation, oxidative stress, and direct toxicity via generation of ROS.<sup>32</sup> Therefore, we focused on the target genes NOX4, COX2 and PGFS, which have high binding energy to Rhein and are associated with oxidative stress and inflammation. To further observe how NOX4, COX2 and PGFS bind to Rhein, PyMOL software was used to show their binding sites to Rhein. As shown in Figure 4A–C, Rhein interacted with ARG338, LYS-340 and ARG-336 of NOX4, ARG-44, GLY-45, CYS-41, TYR-130 and LYS-137 of COX2, and ASN-273, ARG-276, SER-271, LYS-33, TYR-272 and LYS-270 of PGFS through hydrogen bonds. To further validate the binding of Rhein to NOX4, COX2 and PGFS, we performed the CETSA in HK2 cells (Figure 4D). The thermal stability of human NOX4, COX2 and PGFS in the Rhein-treated HK2 cells was decreased with the increased temperatures (37 to 87°C). However, compared with DMSO, Rhein enhanced the thermal stability of NOX4 (Aggregation Temperature ( $T_m$ ) from 54.4°C to 64.2°C), COX2 ( $T_m$  60.7°C to 66.8°C) and PGFS ( $T_m$  from 47.8°C to 56.9°C), and increased their melting points (Figure 4D), likely indicating a direct interaction between Rhein and NOX4, COX2 and PGFS. Moreover, we selected five GSE datasets from the GEO database as external validation sets to confirm the upregulation of NOX4, COX2 and PGFS in kidneys or HK2 cells. As shown in Figure 4E, NOX4, COX2 and PGFS were highly expressed in kidney cortex from CDDP-treated mice/rat or human renal proximal tubular epithelial cells (RPTECs).

Based on molecular docking and CETSA results, MD simulations were conducted to elucidate the protein-ligand stability and protein structural flexibility between Rhein and the three core target proteins NOX4, COX2 and PGFS. During the process of simulation, the RMSD of the NOX4, COX2 and PGFS protein structure was stable, and the RMSD of the compound was stable within 40–50 ns, which indicated that Rhein-NOX4, Rhein-COX2 and Rhein-PGFS could be stably bound (Figure 5A, E and I). The RMSF, which represents the average change in atomic positions over time, was used to characterize the flexibility and movement intensity of protein amino acids throughout the simulation. RMSF value fluctuated steadily below 0.4 nm, indicating that the gyration radius of the protein was stable (Figure 5B, F and J). The radius of gyration ( $R_g$ ) analysis (Figure 5C, G and K) was used to identify the stability of the complex and the results showed that both NOX4, COX2 and PGFS complexes were stable. In addition, the solvent-accessible surface area (SASA) values of the protein-ligand complex remained stable after 20 ns, indicating a strong binding affinity (Figure 5D, H and L).

## Rhein Reduces CDDP-Induced Oxidative Stress, Apoptosis, and Inflammatory Response in the Kidney of Mice

To examine the potential role of Rhein in preventing CDDP-induced AKI, Rhein (80 mg/kg/day) was administered by oral gavage for three consecutive days in mice after intraperitoneal injection with a single dose of CDDP (20 mg/kg) (Figure 6A). Compared to the control group, mice that were injected with CDDP alone exhibited a significant reduction

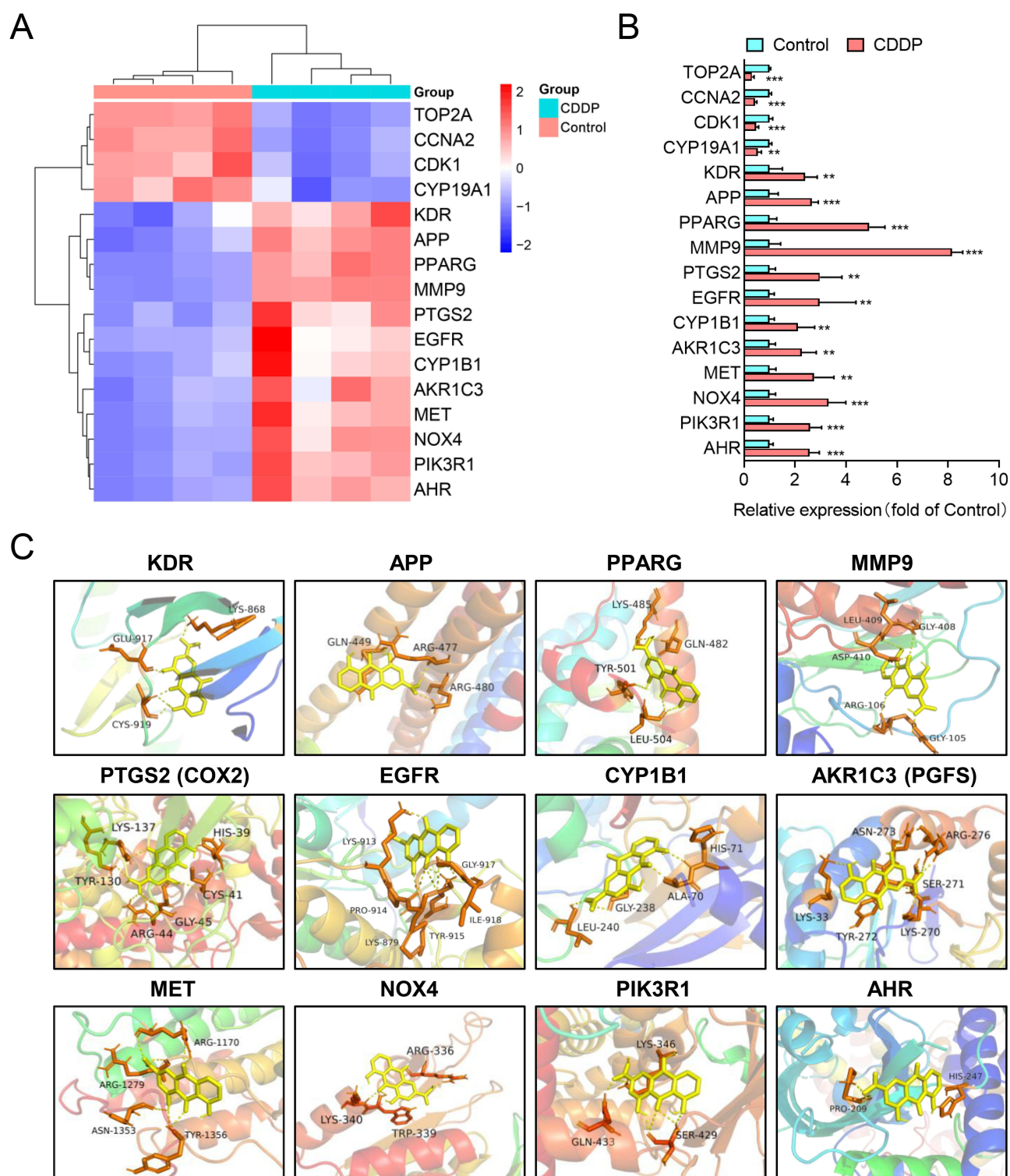


**Figure 3** The expression levels of target genes and the molecular docking between Rhein and proteins encoded by target genes. **(A)** The heatmap of the target genes regulated by Rhein in CDDP-induced human kidney organoids injury model (GSE145085). **(B)** The relative expression of 16 key genes, with 12 high expression and 4 low expression genes. **(C)** Molecular docking between Rhein and the proteins encoded by the 12 target genes. Data are shown as mean  $\pm$  SEM. \*\* $P < 0.01$ , \*\*\* $P < 0.001$ : CDDP vs Control.

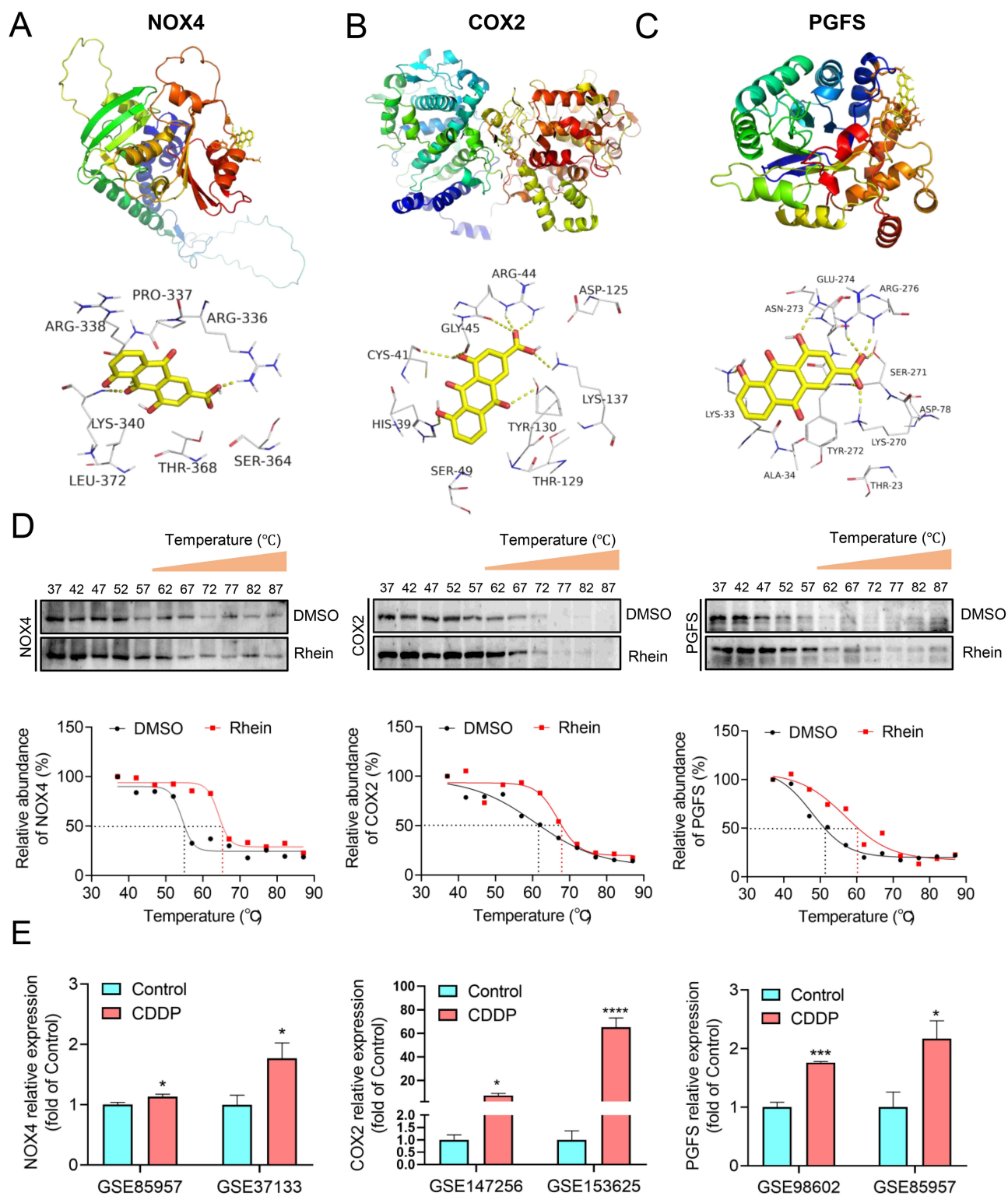


**Figure 4** Molecular docking of Rhein with NOX4, COX2 and PGFS as well as CETSA and database validation. **(A–C)** A structural view of the interaction of Rhein with NOX4, COX2 and PGFS. Rhein is shown as a yellow stick representation. Details on the binding site interactions are shown in the down panel. Non-polar hydrogen atoms are hidden for clarity. Potential intermolecular hydrogen bonds are shown as yellow dashed lines. **(D)** Rhein treatment (40  $\mu$ M) increases the thermal stability of NOX4, COX2 and PGFS in cell lysates as measured by the temperature-dependent cellular thermal shift assay. **(E)** External validation datasets were obtained from transcriptome sequencing data of renal cortical in CDDP-induced AKI or CDDP-treated HK2 cells, including GEO datasets GSE85957, GSE37133, GSE147256, GSE153625 and GSE98602. Data are shown as mean  $\pm$  SEM. Data are shown as mean  $\pm$  SEM. \* $P$  < 0.05, \*\*\* $P$  < 0.001, \*\*\*\* $P$  < 0.0001: CDDP vs Control.

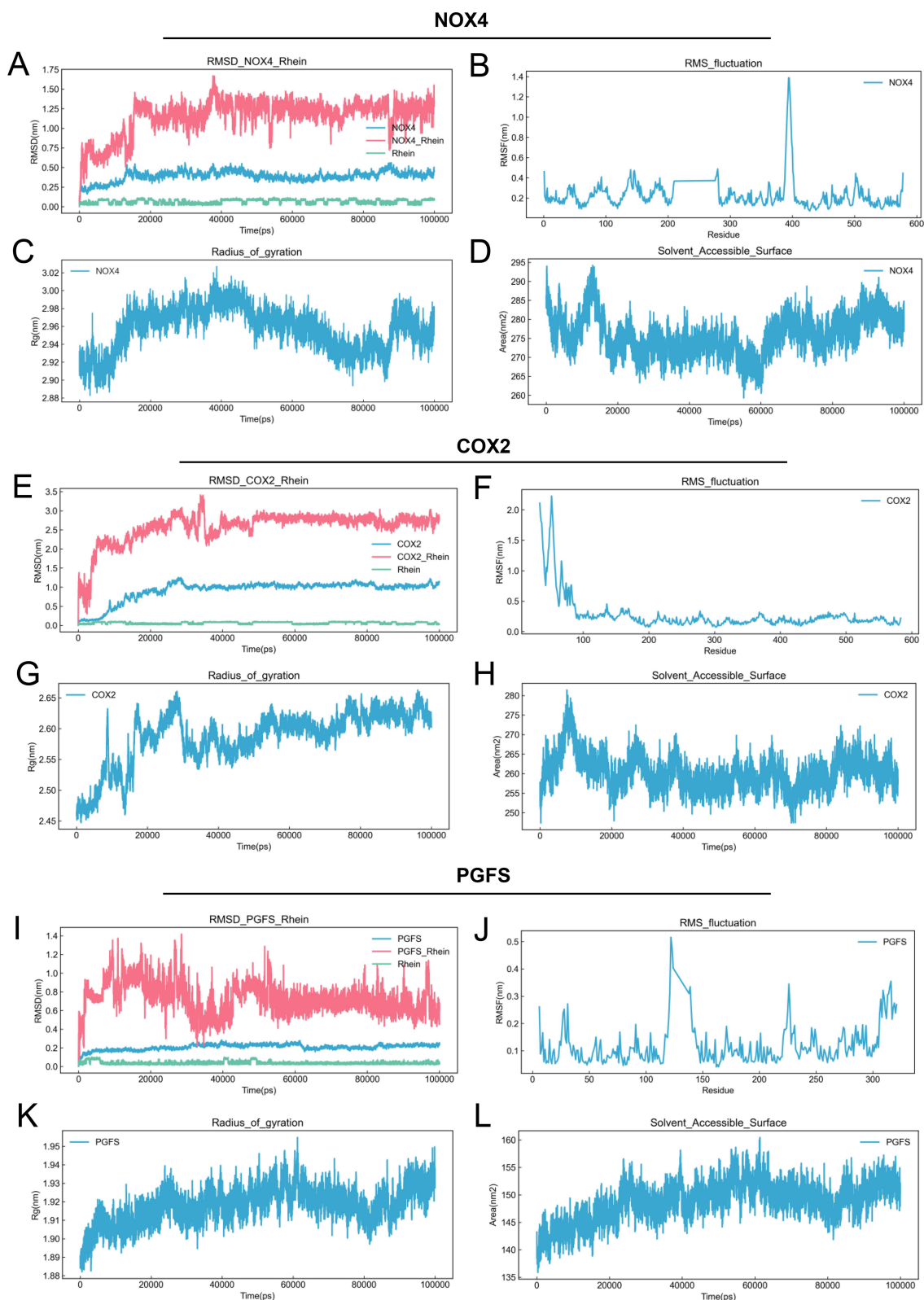


**Figure 5** Molecular dynamic (MD) simulations of Rhen with NOX4, COX2 and PGFS. **(A)** Root-mean-square deviation (RMSD) curve of legend (Rhein, green line), protein (NOX4, blue line), and the NOX4-Rhein complex (red line). **(B)** Root-mean-square fluctuation (RMSF) curve of NOX4. **(C)** Radius of gyration (Rg) curve of NOX4. **(D)** Analysis of solvent accessible surface area (SASA) curve of NOX4. **(E)** RMSD curve of legend (Rhein, green line), protein (COX2, blue line), and the COX2-Rhein complex (red line). **(F)** RMSF curve of COX2. **(G)** Rg curve of COX2. **(H)** SASA curve of COX2. **(I)** RMSD curve of legend (Rhein, green line), protein (PGFS, blue line), and the PGFS-Rhein complex (red line). **(J)** RMSF curve of PGFS. **(K)** Rg curve of PGFS. **(L)** SASA curve of PGFS.

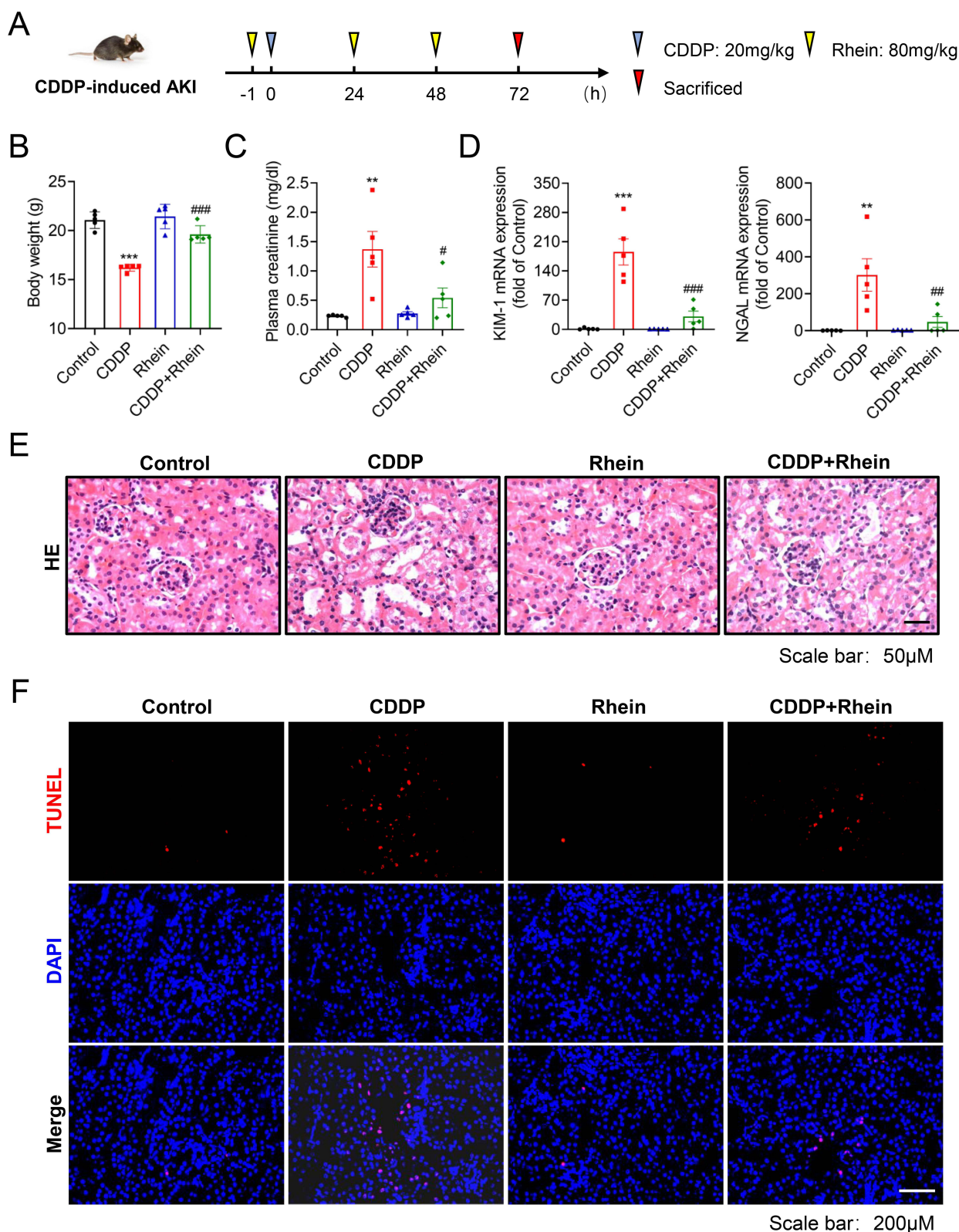


**Figure 6** Rhein reduces CDDP-induced nephrotoxicity. **(A)** A single dose of CDDP (20 mg/kg, i.p.) was administered to the C57BL/6 mice to induce acute kidney injury, and Rhein (80 mg/kg/day) was administered by oral gavage for three consecutive days in mice after intraperitoneal injection with CDDP. **(B)** Changes in body weight were shown ( $n = 5$ ). **(C)** Biochemical determinations of PCr level ( $n = 5$ ). **(D)** Kidney injury molecular-1 (KIM-1) and neutrophil gelatinase-associated lipocalin (NGAL) mRNA expression in renal cortex were determined by qPCR ( $n = 5$ ). **(E)** Representative hematoxylin-eosin (HE) staining was used to evaluate tubular cell necrosis and shedding, tubular lumen dilation and casts ( $n = 5$ ). Scale bars, 50  $\mu$ m. **(F)** Representative TUNEL staining images in renal tissues (DAPI: blue, TUNEL: red) ( $n = 5$ ). Scale bars, 200  $\mu$ m. Data are shown as mean  $\pm$  SEM. \*\*\* $p < 0.01$ , \*\*\*\* $p < 0.001$ : CDDP vs Control. # $p < 0.05$ , ### $p < 0.01$ , #### $p < 0.001$ : CDDP+Rhein vs CDDP.

in body weight and an elevated plasma creatinine (Pcr) level (Figure 6B and C), which was remarkably attenuated by Rhein treatment. There were no significant differences in the body weight and Pcr level between the control and Rhein treatment groups (Figure 6B and C). Kidney injury molecular-1 (KIM-1) and neutrophil gelatinase-associated lipocalin (NGAL) are biomarkers of tubular injuries. As shown in Figure 6D, KIM-1 and NGAL mRNA levels were significantly increased after CDDP injection, which was reversed by Rhein treatment.

As shown in Figure 6E, H&E staining showed kidney lesions in CDDP treated mice, including tubular cell necrosis and shedding, tubular lumen dilation and casts. Interestingly, Rhein remarkably alleviated these changes caused by CDDP. TUNEL staining revealed marked apoptosis in the cortex area after CDDP treatment, but the apoptosis of renal cortex was significantly attenuated by Rhein treatment (Figure 6F).

Western blotting was performed to assess the expression of target protein of Rhein, as well as marker expression of apoptosis and inflammation in the kidney cortex. As shown in Figure 7A, the abundance of NOX4, COX2 and PGFS was markedly increased in renal cortex from CDDP-treated group, which was significantly prevented by Rhein administration. Notably, Western blot analysis showed that CDDP promoted the phosphorylation of p65 and I $\kappa$ B $\alpha$ , potentially indicating an increased NF- $\kappa$ B activation and inflammatory response (Figure 7B). In addition, a downregulation of anti-apoptotic protein Bcl2 was observed in the kidney of CDDP-treated mice, while a concomitant increase in expression level of BAX and cleaved-caspase-3 protein was noted (Figure 7C). The administration of Rhein significantly inhibited the phosphorylation of p65 and prevented apoptosis in the kidney of CDDP mice (Figure 7B and C). These results suggested that Rhein could prevent CDDP-induced AKI in mice.

## Rhein Reduces CDDP-Induced Oxidative Stress, Inflammation and Apoptosis in HK2 Cells

CDDP was administered to HK2 cells at a concentration of 10  $\mu$ M for 24 h to establish the CDDP-induced HK2 cell injury model.<sup>27</sup> Rhein at 40  $\mu$ M significantly increased cell viability, while Rhein at concentrations of 5, 10, 20  $\mu$ M had no effect on CDDP treated HK2 cells (Figure 8A). Thus, 40  $\mu$ M Rhein was selected in the subsequent experiments. Compared with the CDDP treatment group, Rhein significantly reduced the HK2 cell damage caused by CDDP, including the loss of the normal physiological state of oval cells and orderly arrangement (Figure 8B). TUNEL stain and flow cytometric analysis revealed that Rhein significantly prevented CDDP-induced apoptosis (Figure 8C and D) and increased ROS levels (Figure 8E) in HK2 cells, respectively.

As shown in Figure 9A, NOX4, COX2 and PGFS protein abundance were dramatically increased in CDDP-treated HK2 cells, which was markedly prevented by Rhein treatment. CDDP is widely recognized as an inducer of ROS, and given that ROS acts as an effector of NOX4, therefore, the high expression of NOX4 in CDDP-treated HK2 cells is not surprising. Consistent with the findings from TUNEL assays, Rhein effectively inhibited the upregulation of pro-apoptotic proteins Bax and cleaved-caspase 3 abundance, as well as decreased the expression of the antiapoptotic protein Bcl2 in HK2 cells exposed to CDDP (Figure 9B). It was documented that ROS can directly facilitate NF- $\kappa$ B activation.<sup>33–35</sup> As we expected, Rhein inhibited NF- $\kappa$ B activation in CDDP-treated HK2 cells, as evidenced by the reduced levels of phosphorylated p65 and I $\kappa$ B $\alpha$  (Figure 9C). This was consistent with the data described in Figure 2E, HALLMARK enrichment analysis highlighted the significance of the TNFA signaling pathway, which was associated with NF- $\kappa$ B, although TNF $\alpha$  was not the main point we focused on. These findings collectively suggest that Rhein ameliorates CDDP-induced injury and inflammation in HK2 cells, at least in part, through the inhibition of NOX4- NF- $\kappa$ B-COX2/PGFS signaling pathways.

## Rhein Reduces CDDP-Induced Nephrotoxicity without Affecting the Antitumor Efficacy

Determining the impact of Rhein on the antitumor efficacy of CDDP is crucial. We used CDDP-sensitive human non-small-cell lung cancer (NSCLC) cell line A549 to examine the effective of Rhein in vitro. As shown in Figure 10A, Rhein did not affect the anticancer activity of CDDP in A549 cells. When CDDP and Rhein were used together, the anti-tumor effect of CDDP was notably amplified, as seen decreased cell viability. The same effects were also observed in

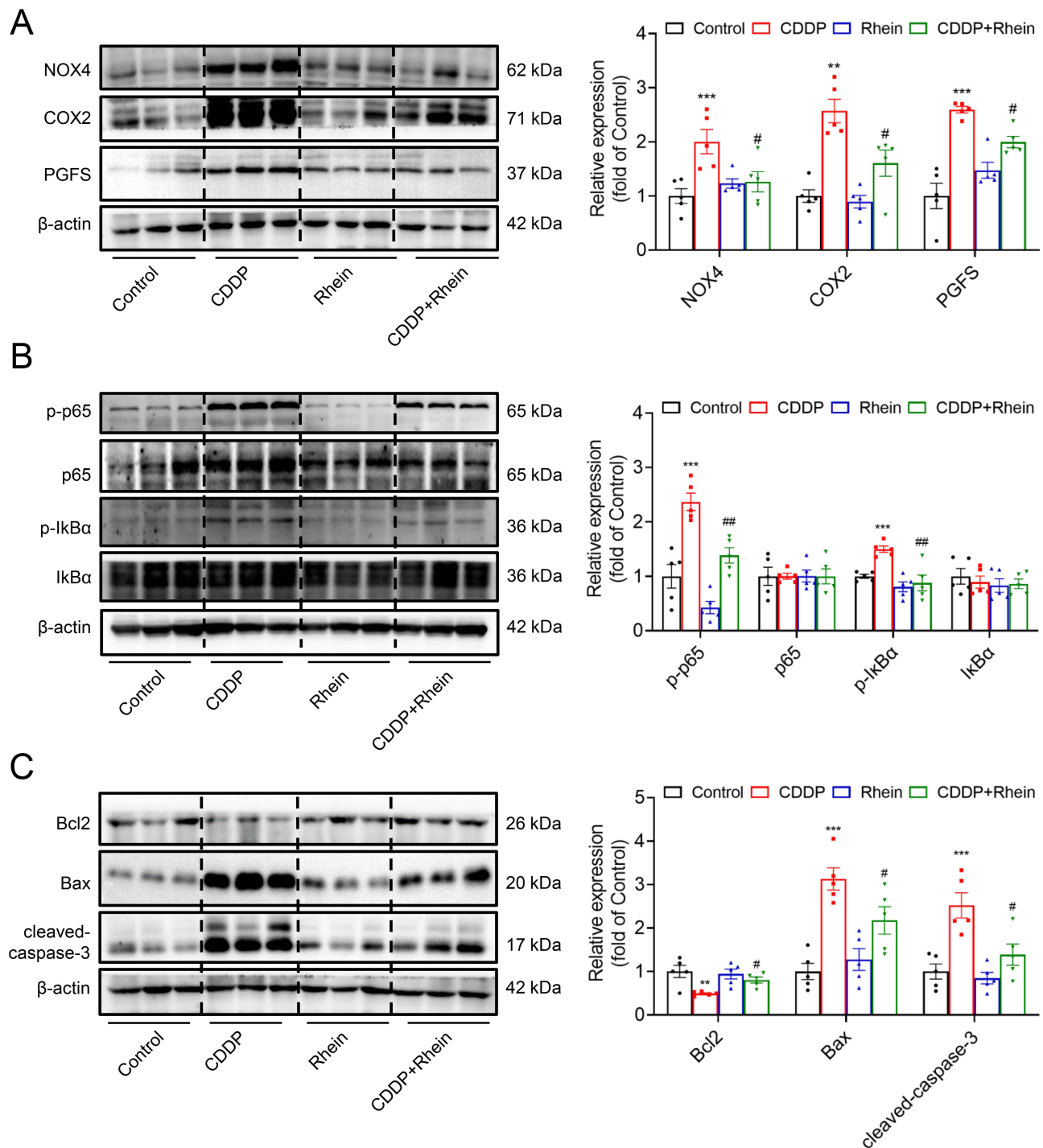


**Figure 7** Rhein reduces CDDP-induced AKI by targeting inhibition of NOX4, COX2 and PGFS. A single dose of CDDP (20 mg/kg, i.p.) was administered to the C57BL/6 mice to induce acute kidney injury, and Rhein (80 mg/kg/day) was administered by oral gavage for three consecutive days in mice after intraperitoneal injection with CDDP. **(A)** NOX4, COX2 and PGFS in renal cortex were measured by Western blot and corresponding quantification analysis (n = 5). **(B)** NF-κB activation-related proteins p-p65/p65 and p-IκBα/ IκBα in renal cortex were measured by Western blot and corresponding quantification analysis (n = 5). **(C)** Apoptosis -related proteins p-p65/p65, Bcl2, BAX and cleaved-caspase-3 in renal cortex were measured by Western blot and corresponding quantification analysis (n = 5). Data are shown as mean ± SEM. \*\**P* < 0.01, \*\*\**P* < 0.001: CDDP vs Control. #*P* < 0.05, ###*P* < 0.01: CDDP+Rhein vs CDDP.

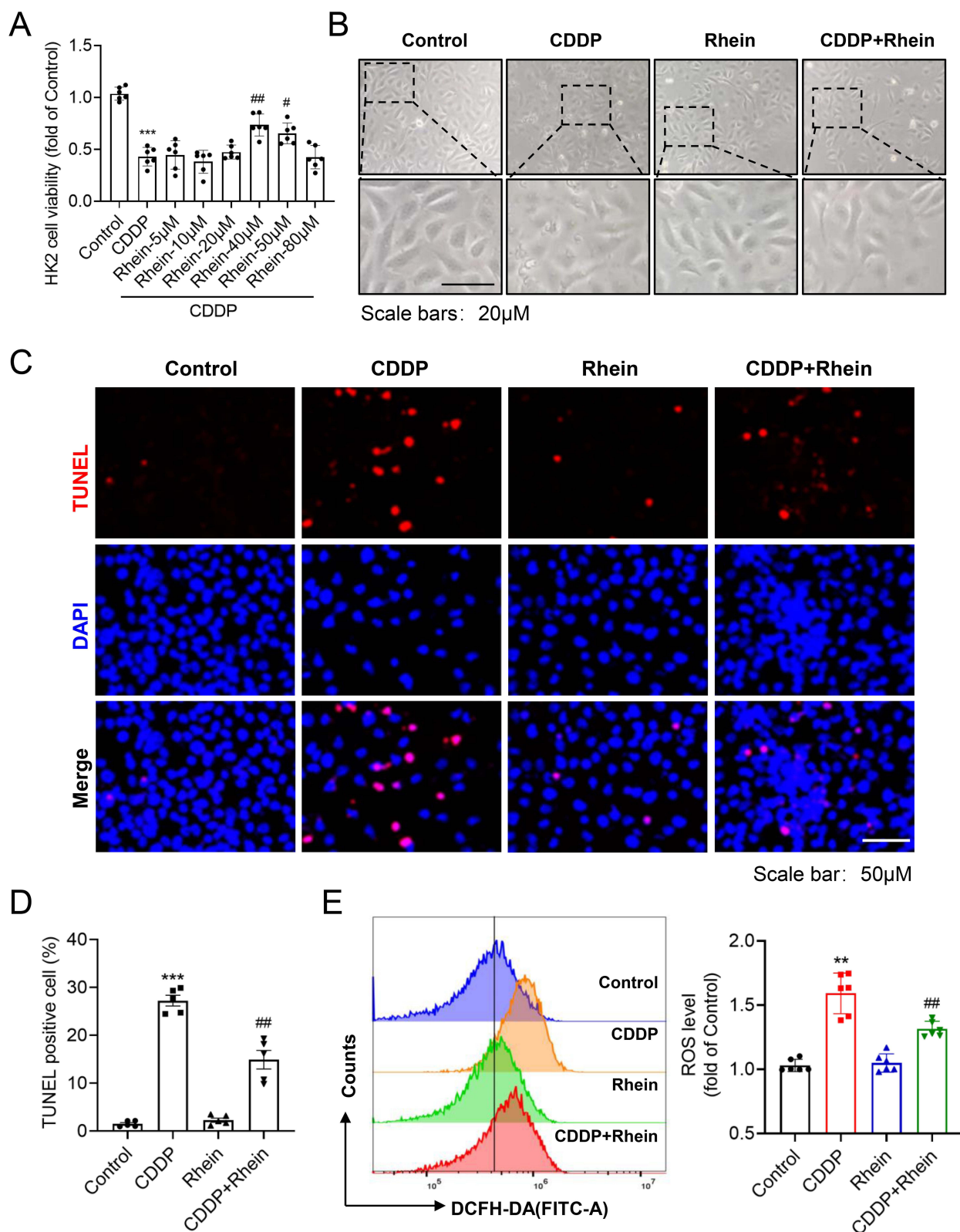


**Figure 8** Rhein reduces CDDP-induced apoptosis and oxidative stress in HK2 cells. CDDP was administered to HK2 cells at a concentration of 10 µg/mL for 24 h to establish the CDDP-induced HK2 cell injury model. **(A)** CDDP-treated HK2 cells were incubated with different concentrations of Rhein for 24 h. The cell viability was determined by the CCK8 analysis (n=6). **(B)** CDDP-treated HK2 cells were incubated with 40 µM Rhein for 24 h. Cellular morphological changes were visualized using an optical microscopy. Scale bars, 20 µm. **(C and D)** Representative TUNEL staining images in HK2 cells (DAPI: blue, TUNEL: red), with corresponding quantification data (n = 5). Scale bars, 50 µm. **(E)** The ROS levels of HK2 cells was determined by flow cytometry analysis (n = 6). Data are shown as mean ± SEM. \*\**P* < 0.01, \*\*\**P* < 0.001: CDDP vs Control. #*P* < 0.05, ###*P* < 0.01: CDDP+Rhein vs CDDP.

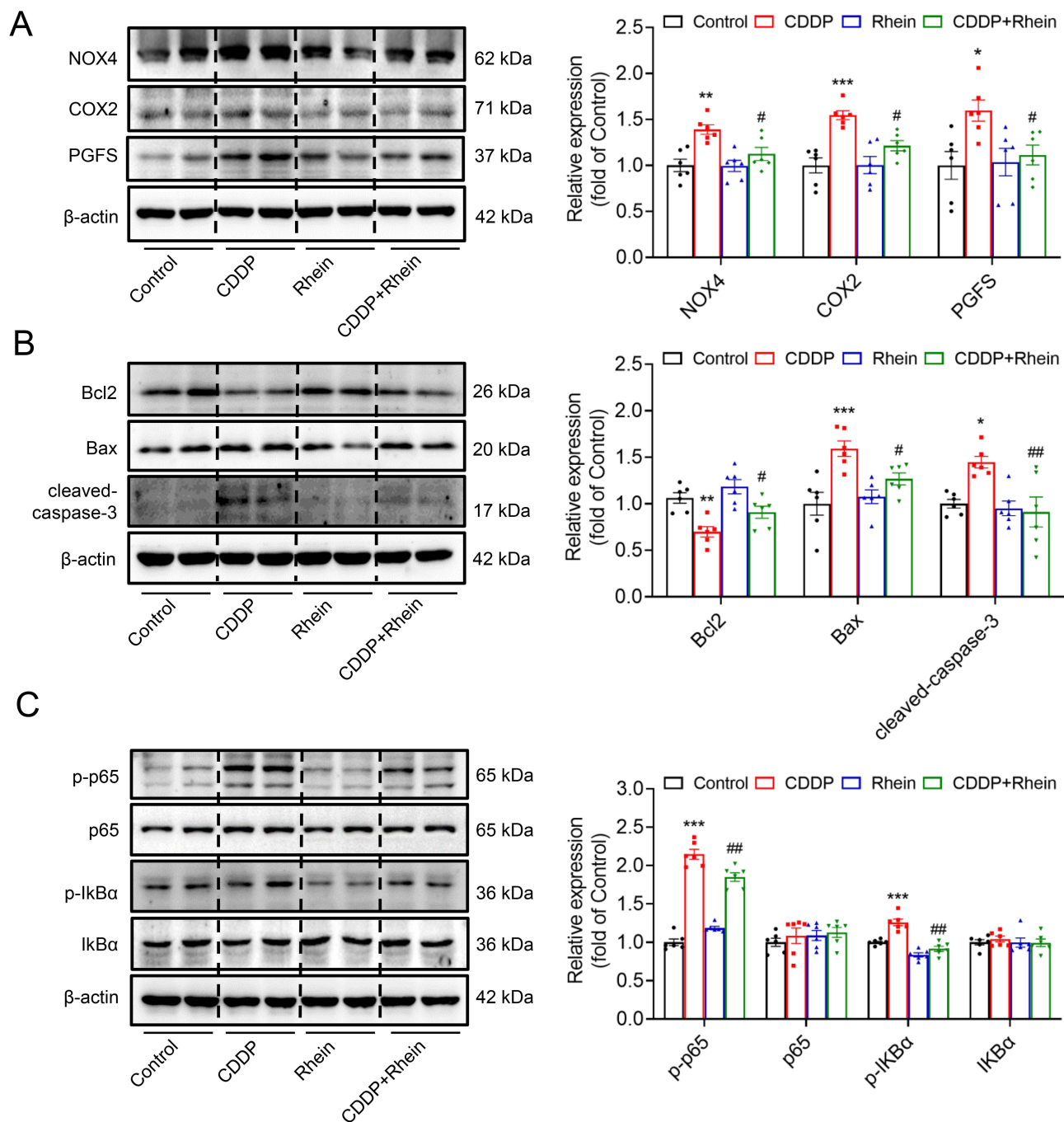


**Figure 9** Rhein mitigated CDDP-induced HK2 cell damage at least in part by downregulation of NOX4-NF- $\kappa$ B-COX2/PGFS signaling pathway. CDDP (10 $\mu$ g/mL)-treated HK2 cells were incubated with 40  $\mu$ M Rhein for 24 h. **(A)** NOX4, COX2 and PGFS in HK2 cells were measured by Western blot and corresponding quantification analysis (n = 6). **(B)** Anti-apoptotic protein Bcl2, and pro-apoptotic proteins BAX and cleaved-caspase-3 in HK2 cells were measured by Western blot and corresponding quantification analysis (n = 6). **(C)** NF- $\kappa$ B activation-related proteins p-p65/p65 and p-IkBa/ IkBa in HK2 cells were measured by Western blot and corresponding quantification analysis (n = 6). Data are shown as mean  $\pm$  SEM. \* $P$  < 0.05, \*\* $P$  < 0.01, \*\*\* $P$  < 0.001: CDDP vs Control. # $P$  < 0.05, ## $P$  < 0.01: CDDP+Rhein vs CDDP.

lewis (LLC) tumor-bearing mice treated with Rhein and CDDP *in vivo*. The combined treatment with CDDP and Rhein on mice bearing tumors had better antitumor effect (weight and size of tumors) than CDDP alone (Figure 10B–D). These results suggest that Rhein likely strengthens the anti-cancer efficacy of CDDP and at the same time prevents adverse effects of CDDP in the kidney.

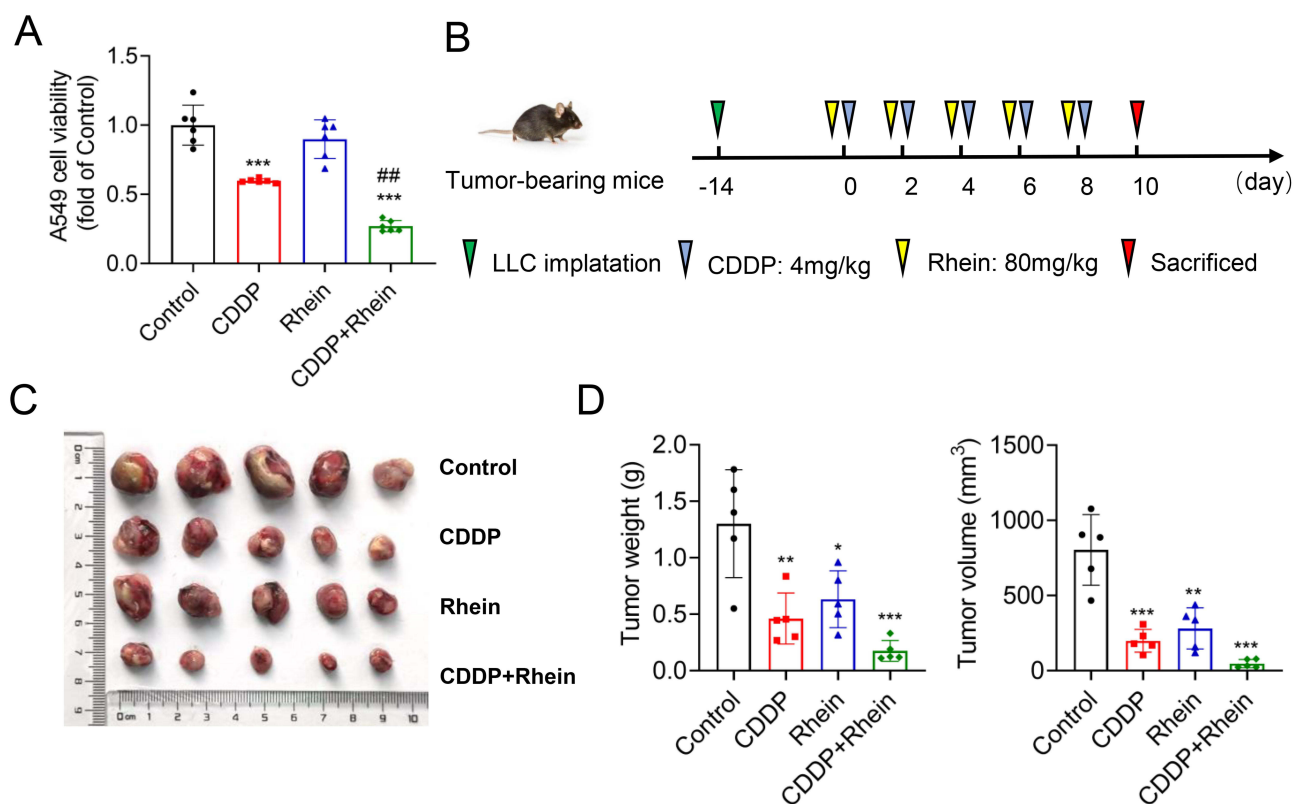


**Figure 10** Rhein reduces CDDP-induced nephrotoxicity without affecting the antitumor efficacy. CDDP (10 $\mu$ M)-treated human non-small-cell lung cancer (NSCLC) A549 cells were incubated with 40  $\mu$ M Rhein for 24 h. **(A)** The cell viability was determined by the CCK8 analysis (n=6). **(B)** The CDDP-sensitive Lewis lung carcinoma (LLC) cells ( $2 \times 10^5$ ) were inoculated subcutaneously into C57BL/6 mice for 14 days, and the mice were treated with CDDP alone (4 mg/kg, the drugs were administered every other day for 10 days, resulting in an accumulative dose of 20 mg/kg) or combination with Rhein (80mg/kg, the drugs were administered 1 hour after CDDP injection). **(C and D)** The xenograft tumor weights and tumor volume of C57BL/6 mice injected subcutaneously with LLC cells with the treatment of CDDP, Rhein alone or in combination with Rhein (n=5). Data are shown as mean  $\pm$  SEM. \* $P < 0.05$ , \*\* $P < 0.01$ , \*\*\* $P < 0.001$ : CDDP vs Control. ## $P < 0.01$  CDDP+Rhein vs CDDP.

## Discussion

AKI is a global disease with a poor prognosis. At present, there is no available treatment to prevent CDDP-induced AKI.<sup>36</sup> Effective treatments for CDDP-induced nephrotoxicity are therefore urgently needed. Although *Radix Rhein Et Rhizome* has a wide range of pharmacological activities, its complex chemical composition makes it difficult to elucidate its potential active compounds and pharmacological mechanisms. In the present study, we presented direct evidence that Rhein, one of the active components from *Radix Rhein Et Rhizome*, alleviates CDDP-induced kidney damage by network pharmacology and validation of in vitro and in vivo experiments. We have demonstrated that the protective effects of Rhein on CDDP-induced AKI could be, at least in part, attributed to targeting inhibition of NOX4-COX2/PGFS axis.

A combination of network pharmacology, molecular docking, MD simulations and experimental validation was performed to systematically investigate the bioactive components of *Radix Rhein Et Rhizome* and its therapeutic mechanism for AKI in this research. Many overlapping targets were found in different compounds of *Radix Rhein Et Rhizome*, indicating that *Radix Rhein Et Rhizome* exerts renoprotective properties through the synergistic effect of its compounds. In addition to Rhein, beta-sitosterol and Aloe-emodin are also the main active components of *Radix Rhein Et Rhizome* (Figure 1A). For example,  $\beta$ -sitosterol is recently shown to be a novel drug for alleviating cardiac and renal complications of acute renal ischemia-reperfusion injury with great therapeutic potential<sup>37</sup> and a potential herbal nutraceutical for diabetic management.<sup>38</sup> Aloe-emodin exhibits beneficial properties such as antioxidative, anti-inflammatory and anticarcinogenic activities in various diseases.<sup>39–41</sup> Aloe-emodin was shown to protect against fibrosis in UUO kidneys,<sup>42</sup> but in another study Aloe-emodin induced apoptosis of HK2 cells through endoplasmic reticulum stress.<sup>43</sup> Considering the multi-component and multi-target characteristics of TCM,<sup>44</sup> these key active ingredients are worthy of further investigation.

In the current study, we focused on Rhein, one of the active ingredients from *Radix Rhein Et Rhizome*, which plays a protective role in CDDP-induced AKI, as Rhein has anticancer and renoprotective properties.<sup>15,45</sup> GO and HALLMARK enrichment analyses revealed that Rhein prevented development of AKI mainly through inhibiting ROS, inflammatory responses and apoptosis-associated signaling pathways. The abnormal activation of these targets in tubular epithelial cells may promote the development of AKI through triggering apoptosis, oxidative stress and inflammation. In the PPI analysis, we found that 16 genes including NOX4, COX2 and PGFS are the core targets of Rhein in the prevention and treatment of CDDP-induced AKI. By molecular docking and MD simulations, it was further identified that the proteins encoded by the above three genes could bind to Rhein with high affinity. NOX4-mediated ROS production was also known to be the activator of NF- $\kappa$ B, a transcriptional factor mediating inflammatory responses.<sup>34,46,47</sup> In CDDP-treated mice, high expression of the target proteins (including NOX4, COX2 and PGFS) and phosphorylated-p65/ I $\kappa$ B $\alpha$  in the cortex were reduced by Rhein. In HK2 cells, we found that the NOX4-mediated ROS was associated with increased NF- $\kappa$ B phosphorylation, presumably inducing inflammatory responses, while Rhein inhibits ROS levels. Our in vitro and in vivo data therefore confirmed the predictive power of network pharmacology and suggested that Rhein can prevent CDDP-induced AKI, likely through its anti-apoptotic and cytoprotective property by inhibiting the NOX4-NF- $\kappa$ B-COX2/PGFS axis.

To date, although the pathophysiological basis of CDDP nephrotoxicity has been widely studied, the molecular mechanism of CDDP-induced renal injury has not been clarified yet and may involve multiple signaling pathways and genes. Our bioinformatics analysis identified significant upregulation of multiple genes (eg CYP1B1, PIK3R1, AHR, NOX4, COX2, and PGFS) in the CDDP-induced nephrotoxicity model, all demonstrating strong binding affinity to Rhein. CYP1B1 and AHR are well-characterized in xenobiotic metabolism (eg, drug detoxification) and are highly expressed in the liver,<sup>48,49</sup> although their renal expression is detectable, their primary roles involve ligand-activated transcriptional regulation of detoxifying enzymes (eg, CYP1 family).<sup>50</sup> The upregulation of CYP1B1 and AHR in our model likely reflects a generalized stress response to CDDP rather than kidney-specific toxicity mechanisms. PIK3R1, while ubiquitously expressed, is predominantly involved in metabolic regulation (eg, insulin signaling) and tumor resistance/metastasis.<sup>51,52</sup> Based on these functional considerations, we strategically prioritized investigation of NOX4, COX2, and PGFS as mechanistically relevant candidates for CDDP nephrotoxicity but not the other three proteins described above.

GO and HALLMARK pathway enrichment analyses revealed predominant activation of oxidative stress and inflammatory pathways in CDDP-induced nephrotoxicity, showing mechanistic convergence with our three candidate genes (NOX4, COX2, and PGFS). The upregulation of NOX4 protein expression is associated with increased oxidative stress.<sup>9</sup> NOX4 could also activate NF- $\kappa$ B pathway, upregulating the inflammatory factors and inducing oxidative stress.<sup>34,35</sup> In the process of inflammation, COX2 is a key molecule highlighted by our experiments. COX2 expression and PGE2 release have been shown to be dependent on activation of the transcription factor NF- $\kappa$ B.<sup>53</sup> Given its primary anti-inflammatory and antioxidant properties, it is unsurprising that Rhein is capable of modulating the NOX4 and COX2-mediated pathways. In addition to COX2, PGFS is also a key molecule in the prostaglandin synthesis pathway, which acts downstream of COX2 and is involved in maintaining prostaglandin synthesis and regulating inflammatory response.<sup>54</sup> Importantly, Rhein exhibited a very high docking potential with PGFS and COX2, especially with PGFS, compared to other target proteins ([Table S4](#)), suggesting that its protective effects may be primarily attributed to regulating inflammatory responses through multiple pathways. Indeed, recent studies have also shown that Rhein can improve uric acid nephropathy and kidney fibrosis by targeting the inhibition of inflammatory pathways,<sup>19,55</sup> consistent with our findings. Interestingly, study have shown that AKR1C3 increased NF- $\kappa$ B activity by interacting with TRAF6, and NF- $\kappa$ B activation results in the release of inflammatory mediators (IL1b, IL6, and TNF $\alpha$ ).<sup>56</sup> Therefore, in this study, AKR1C3-driven NF- $\kappa$ B activation may also form a positive feedback loop mediating kidney inflammation. From the overall perspective, the pathways which are related to the targets of Rhein, are initiated by the membrane receptor,<sup>16</sup> with NOX4 in this study serving as excellent examples. The therapeutic effect of Rhein, as a multitarget compound, is the synergistic and comprehensive involvement of multiple pathways rather than the blocking or activating one single signaling pathway.<sup>57</sup> Therefore, in addition to the target proteins/genes involved in oxidative stress and inflammation, other molecules may also participate in the pathways through which Rhein exerts renal protective effects, apparently, further experiments are still warranted.

Our molecular docking results demonstrated that Rhein exhibits strong binding affinities with the catalytic sites of NOX4 (−8.9 kcal/mol), COX2 (−8.6 kcal/mol), and PGFS (−10.4 kcal/mol), with binding energies indicating thermodynamically favorable interactions. These negative  $\Delta G$  values reflect optimal structural complementarity between the ligand and receptor binding pockets, suggesting stable complex formation through coordinated hydrogen bonding, hydrophobic interactions or electrostatic forces. Molecular docking established systematic identification of Rhein's binding modes within these enzymatic active sites, revealing critical molecular determinants for its potential inhibitory effects.

Complementing these static analyses, we conducted all-atom molecular dynamics simulations to investigate the dynamic stability of Rhein-protein complexes under near-physiological conditions. These simulations tracked conformational evolution for 100 ns, evaluating key parameters including RMSD, RMSF, Rg, and SASA. After approximately 40 ns of simulation, the RMSD stabilizes with some fluctuations, suggesting that Rhein likely maintains a high stability at its binding site with the protein. Certain local regions in the RMSF exhibit significant fluctuations, such as near residue 400 of NOX4, residue 50 of COX2, and residue 130 of PGFS, where the RMSF values reach remarkable peaks. This indicates that these areas may be critical functional regions of the protein following the binding of Rhein to NOX4, COX2, and PGFS. These regions are likely to be flexible loop regions of the protein or functional areas directly interacting with Rhein. Our subsequent CETAS data, along with validation at the animal and cellular levels, suggest that Rhein likely exerts its inhibitory effects on CDDP-induced renal oxidative stress and inflammation at least partially through the inhibition of NOX4, COX2, and PGFS.

## Conclusion

In conclusion, we identified the core targets and critical pathways of Rhein against CDDP-induced AKI using a pharmacological approach and bioinformatic analysis, validated by *in vivo* and *in vitro* studies. We believed that Rhein attenuates CDDP-induced kidney damage likely by downregulating NOX4-COX2/PGFS axis. These data likely indicate that Rhein may be a potentially therapeutic option for CDDP-induced AKI.

## Abbreviations

AKI, Acute kidney injury; AHR, aryl hydrocarbon receptor; APP, amyloid beta precursor protein; AKR1C3 (PGFS), aldo-keto reductase family 1 member C3; CDDP, cis-diamminedichloroplatinum II (Cisplatin); CYP1B1, cytochrome P450 family 1 subfamily B member 1; DEGs, Differentially expressed genes; EGFR, Epidermal growth factor receptor; KDR, kinase insert domain receptor; KIM-1, Kidney injury molecular-1; MD, molecular dynamic; MET, MET proto-oncogene, receptor tyrosine kinase; MMP9, matrix metalloproteinase 9; NGAL, Neutrophil gelatinase-associated lipocalin; NOX4, NADPH oxidase 4; PIK3R1, phosphoinositide-3-kinase regulatory subunit 1; PPAR $\gamma$ , peroxisome proliferator activated receptor gamma; PTGS2 (COX2), prostaglandin-endoperoxide synthase 2; PCr, Plasma creatinine; Radius of gyration, Rg; Root-mean-square deviation, RMSD; RMSF, Root-mean-square fluctuation; Solvent-accessible surface area, SASA; TCM, Traditional Chinese medicine; UUO, unilateral ureteral obstruction.

## Data Sharing Statement

The data that support the findings of this study are available on request from the corresponding author upon reasonable request.

## Ethics Statement

This study strictly adhered to international and national ethical standards for both human data usage and animal experimentation. All experimental procedures involving animals were performed in full compliance with the Guidelines for the Ethical Review of Laboratory Animal Welfare (China, GB/T 35892-2018) and were approved by the Institutional Animal Care and Use Committee (IACUC) of Sun Yat-sen University (Approval No. 2023001813). Animal care and use protocols followed the standards set by the Association for Assessment and Accreditation of Laboratory Animal Care International (AAALAC). Research involving human data was reviewed and approved by the Institutional Review Board (IRB) of Zhongshan School of Medicine, Sun Yat-sen University. The study utilized only de-identified, publicly available datasets from which all personally identifiable information (eg, names, addresses) had been

removed, retaining only biologically relevant data. These datasets had previously obtained ethical approval and informed consent from participants during their original collection. In accordance with Article 32 (Items 1 and 2) of China's Measures for Ethical Review of Life Science and Medical Research Involving Human Subjects (2023), this secondary analysis of anonymized data qualified for exemption from additional ethical review by our institution.

## Author Contributions

All authors made a significant contribution to the work reported, whether that is in the conception, study design, execution, acquisition of data, analysis and interpretation, or in all these areas; took part in drafting, revising or critically reviewing the article; gave final approval of the version to be published; have agreed on the journal to which the article has been submitted; and agree to be accountable for all aspects of the work.

## Funding

This work was supported by the National Natural Science Foundation of China (Grant Nos. 82170693, 82370679, 82270744), Natural Science Foundation of Guangdong Province (2021A1515011482, 2022A1515010787), and Guangzhou Municipal Science and Technology Bureau (202201011621).

## Disclosure

The authors report no conflicts of interest in this work.

## References

- Ostermann M, Lumlertgul N, Jeong R, See E, Joannidis M, James M. Acute kidney injury. *Lancet*. 2025;405(10474):241–256. doi:10.1016/S0140-6736(24)02385-7
- Mehta RL, Burdmann EA, Cerdá J, et al. Recognition and management of acute kidney injury in the international society of nephrology Oby25 global snapshot: a multinational cross-sectional study. *Lancet*. 2016;387(10032):2017–2025. doi:10.1016/S0140-6736(16)30240-9
- Holditch SJ, Brown CN, Lombardi AM, Nguyen KN, Edelstein CL. Recent advances in models, mechanisms, biomarkers, and interventions in cisplatin-induced acute kidney injury. *Int J Mol Sci*. 2019;20(12):3011. doi:10.3390/ijms20123011
- Tang C, Livingston MJ, Safirstein R, Dong Z. Cisplatin nephrotoxicity: new insights and therapeutic implications. *Nat Rev Nephrol*. 2023;19(1):53–72. doi:10.1038/s41581-022-00631-7
- Horie S, Oya M, Nangaku M, et al. Guidelines for treatment of renal injury during cancer chemotherapy 2016. *Clin Exp Nephrol*. 2018;22(1):210–244. doi:10.1007/s10157-017-1448-z
- Crona DJ, Faso A, Nishijima TF, McGraw KA, Galsky MD, Milowsky MI. a systematic review of strategies to prevent cisplatin-induced nephrotoxicity. *Oncologist*. 2017;22(5):609–619. doi:10.1634/theoncologist.2016-0319
- Jing Q, Zhou C, Zhang J, et al. Role of reactive oxygen species in myelodysplastic syndromes. *Cell Mol Biol Lett*. 2024;29(1):53. doi:10.1186/s11658-024-00570-0
- Gao Y, Lu X, Zhang G, et al. DRD4 alleviates acute kidney injury by suppressing ISG15/NOX4 axis-associated oxidative stress. *Redox Biol*. 2024;70:103078. doi:10.1016/j.redox.2024.103078
- Pecchillo Cimmino T, Ammendola R, Cattaneo F, Esposito G. NOX dependent ROS generation and cell metabolism. *Int J Mol Sci*. 2023;24(3):2086. doi:10.3390/ijms24032086
- Barakat LAA, Barakat N, Zakaria MM, Khirallah SM. Protective role of zinc oxide nanoparticles in kidney injury induced by cisplatin in rats. *Life Sci*. 2020;262:118503. doi:10.1016/j.lfs.2020.118503
- Forrester SJ, Kikuchi DS, Hernandez MS, Xu Q, Griendling KK. Reactive oxygen species in metabolic and inflammatory signaling. *Circ Res*. 2018;122(6):877–902. doi:10.1161/CIRCRESAHA.117.311401
- Lingappan K. NF- $\kappa$ B in oxidative stress. *Curr Opin Toxicol*. 2018;7:81–86. doi:10.1016/j.cotox.2017.11.002
- Ridzuan NRA, Rashid NA, Othman F, Budin SB, Hussan F, Teoh SL. Protective role of natural products in cisplatin-induced nephrotoxicity. *Mini Rev Med Chem*. 2019;19(14):1134–1143. doi:10.2174/1389557519666190320124438
- Fang CY, Lou DY, Zhou LQ, et al. Natural products: potential treatments for cisplatin-induced nephrotoxicity. *Acta Pharmacol Sin*. 2021;42(12):1951–1969. doi:10.1038/s41401-021-00620-9
- Zhu Y, Yang S, Lv L, et al. Research progress on the positive and negative regulatory effects of rhein on the kidney: a review of its molecular targets. *Molecules*. 2022;27(19):6572. doi:10.3390/molecules27196572
- Sun H, Luo G, Chen D, Xiang Z. A comprehensive and system review for the pharmacological mechanism of action of rhein, an active anthraquinone ingredient. *Front Pharmacol*. 2016;7:247. doi:10.3389/fphar.2016.00247
- Song X, Du Z, Yao Z, Tang X, Zhang M. Rhein improves renal fibrosis by restoring cpt1a-mediated fatty acid oxidation through SirT1/STAT3/twist1 pathway. *Molecules*. 2022;27(7):2344. doi:10.3390/molecules27072344
- Wu X, Liu M, Wei G, et al. Renal protection of rhein against 5/6 nephrectomied-induced chronic kidney disease: role of SIRT3-FOXO3 $\alpha$  signalling pathway. *J Pharm Pharmacol*. 2020;72(5):699–708. doi:10.1111/jph.13234
- Hu J, Yang Z, Wu H, Wang D. Rhein attenuates renal inflammatory injury of uric acid nephropathy via lincRNA-Cox2/miR-150-5p/STAT1 axis. *Int Immunopharmacol*. 2020;85:106620. doi:10.1016/j.intimp.2020.106620

20. quan JZ, wen HC, jie LC, wen SW, Chen B, Run TP. Effects of rhein on activity of caspase-3 in kidney and cell apoptosis on the progression of renal injury in glomerulosclerosis. *Zhonghua Yi Xue Za Zhi*. 2005;85(26):1836–1841.
21. Fu S, Zhou Y, Hu C, Xu Z, Hou J. Network pharmacology and molecular docking technology-based predictive study of the active ingredients and potential targets of rhubarb for the treatment of diabetic nephropathy. *BMC Complement Med Ther*. 2022;22(1):210. doi:10.1186/s12906-022-03662-6
22. Robinson MD, McCarthy DJ, Smyth GK. edgeR: a bioconductor package for differential expression analysis of digital gene expression data. *Bioinformatics*. 2010;26(1):139–140. doi:10.1093/bioinformatics/btp616
23. Wu T, Hu E, Xu S, et al. clusterProfiler 4.0: a universal enrichment tool for interpreting omics data. *Innovation*. 2021;2(3):100141. doi:10.1016/j.xinn.2021.100141
24. Hu J, Gu W, Ma N, Fan X, Ci X. Leonurine alleviates ferroptosis in cisplatin-induced acute kidney injury by activating the Nrf2 signalling pathway. *Br J Pharmacol*. 2022;179(15):3991–4009. doi:10.1111/bph.15834
25. Wu J, Wei Z, Cheng P, et al. Rhein modulates host purine metabolism in intestine through gut microbiota and ameliorates experimental colitis. *Theranostics*. 2020;10(23):10665–10679. doi:10.7150/thno.43528
26. Chen X, Liu Y, Wang Y, et al. CYP4F2-catalyzed metabolism of arachidonic acid promotes stromal cell-mediated immunosuppression in non-small cell lung cancer. *Cancer Res*. 2022;82(21):4016–4030. doi:10.1158/0008-5472.CAN-21-4029
27. Song J, Sheng J, Lei J, Gan W, Yang Y. Mitochondrial targeted antioxidant SKQ1 ameliorates acute kidney injury by inhibiting ferroptosis. *Oxid Med Cell Longev*. 2022;2022:2223957. doi:10.1155/2022/2223957
28. Dai L, Prabhu N, Yu LY, Bacanu S, Ramos AD, Nordlund P. Horizontal cell biology: monitoring global changes of protein interaction states with the proteome-Wide Cellular Thermal Shift Assay (CETSA). *Annu Rev Biochem*. 2019;88:383–408. doi:10.1146/annurev-biochem-062917-012837
29. Tu Y, Tan L, Tao H, Li Y, Liu H. CETSA and thermal proteome profiling strategies for target identification and drug discovery of natural products. *Phytomedicine*. 2023;116:154862. doi:10.1016/j.phymed.2023.154862
30. Zhang F, Wu R, Liu Y, et al. Nephroprotective and nephrotoxic effects of Rhubarb and their molecular mechanisms. *Biomed Pharmacother*. 2023;160:114297. doi:10.1016/j.biopha.2023.114297
31. Guo R, Yi Z, Wang Y, Wang L. Network pharmacology and experimental validation to explore the potential mechanism of Sanjie Zhentong Capsule in endometriosis treatment. *Front Endocrinol*. 2023;14:1110995. doi:10.3389/fendo.2023.1110995
32. Digby JLM, Vanichapol T, Przepiorski A, Davidson AJ, Sander V. Evaluation of cisplatin-induced injury in human kidney organoids. *Am J Physiol Renal Physiol*. 2020;318(4):F971–F978. doi:10.1152/ajprenal.00597.2019
33. Burr SD, Stewart JA. Rap1a overlaps the AGE/RAGE signaling cascade to alter expression of  $\alpha$ -SMA, p-NF- $\kappa$ B, and p-PKC- $\zeta$  in cardiac fibroblasts isolated from type 2 diabetic mice. *Cells*. 2021;10(3):557. doi:10.3390/cells10030557
34. Fan L, Xiao Q, Zhang L, et al. CAPE-pNO2 attenuates diabetic cardiomyopathy through the NOX4/NF- $\kappa$ B pathway in STZ-induced diabetic mice. *Biomed Pharmacother*. 2018;108:1640–1650. doi:10.1016/j.biopha.2018.10.026
35. Guan L, Mao Z, Yang S, et al. Dioscin alleviates Alzheimer's disease through regulating RAGE/NOX4 mediated oxidative stress and inflammation. *Biomed Pharmacother*. 2022;152:113248. doi:10.1016/j.biopha.2022.113248
36. Zhu H, Jiang W, Zhao H, et al. PSTPIP2 inhibits cisplatin-induced acute kidney injury by suppressing apoptosis of renal tubular epithelial cells. *Cell Death Dis*. 2020;11(12):1057. doi:10.1038/s41419-020-03267-2
37. Koc K, Geyikoglu F, Cakmak O, et al. The targets of  $\beta$ -sitosterol as a novel therapeutic against cardio-renal complications in acute renal ischemia/reperfusion damage. *Naunyn Schmiedebergs Arch Pharmacol*. 2021;394(3):469–479. doi:10.1007/s00210-020-01984-1
38. Babu S, Jayaraman S. An update on  $\beta$ -sitosterol: a potential herbal nutraceutical for diabetic management. *Biomed Pharmacother*. 2020;131:110702. doi:10.1016/j.biopha.2020.110702
39. Devi G, Harikrishnan R, Paray BA, Al-Sadoon MK, Hoseinifar SH, Balasundaram C. Effects of aloe-emodin on innate immunity, antioxidant and immune cytokines mechanisms in the head kidney leucocytes of Labeo rohita against *Aphanomyces invadans*. *Fish Shellfish Immunol*. 2019;87:669–678. doi:10.1016/j.fsi.2019.02.006
40. Hu B, Zhang H, Meng X, Wang F, Wang P. Aloe-emodin from rhubarb (*Rheum rhabarbarum*) inhibits lipopolysaccharide-induced inflammatory responses in RAW264.7 macrophages. *J Ethnopharmacol*. 2014;153(3):846–853. doi:10.1016/j.jep.2014.03.059
41. Lee PJ, Ho CC, Ho H, et al. Tumor microenvironment-based screening repurposes drugs targeting cancer stem cells and cancer-associated fibroblasts. *Theranostics*. 2021;11(19):9667–9686. doi:10.7150/thno.62676
42. Dou F, Liu Y, Liu L, et al. Aloe-emodin ameliorates renal fibrosis via inhibiting PI3K/Akt/mTOR signaling pathway in vivo and in vitro. *Rejuvenation Res*. 2019;22(3):218–229. doi:10.1089/rej.2018.2104
43. Zhu S, Jin J, Wang Y, et al. The endoplasmic reticulum stress response is involved in apoptosis induced by aloe-emodin in HK-2 cells. *Food Chem Toxicol*. 2012;50(3–4):1149–1158. doi:10.1016/j.fct.2011.12.018
44. Han Y, Sun H, Zhang A, Yan G, Wang XJ. Chinmedomics, a new strategy for evaluating the therapeutic efficacy of herbal medicines. *Pharmacol Ther*. 2020;216:107680. doi:10.1016/j.pharmthera.2020.107680
45. Ma L, Wei HL, Wang KJ, et al. Rhein promotes TRAIL-induced apoptosis in bladder cancer cells by up-regulating DR5 expression. *Aging*. 2022;14(16):6642–6655. doi:10.18632/aging.204236
46. Ryu YS, Kang KA, Piao MJ, et al. Particulate matter induces inflammatory cytokine production via activation of NF $\kappa$ B by TLR5-NOX4-ROS signaling in human skin keratinocyte and mouse skin. *Redox Biol*. 2019;21:101080. doi:10.1016/j.redox.2018.101080
47. Zhang M, Xu Y, Qiu Z, Jiang L. Sulforaphane attenuates angiotensin II-induced vascular smooth muscle cell migration via suppression of NOX4/ROS/Nrf2 signaling. *Int J Biol Sci*. 2019;15(1):148–157. doi:10.7150/ijbs.28874
48. Li F, Zhu W, Gonzalez FJ. Potential role of CYP1B1 in the development and treatment of metabolic diseases. *Pharmacol Ther*. 2017;178:18–30. doi:10.1016/j.pharmthera.2017.03.007
49. Fardel O. Cytokines as molecular targets for aryl hydrocarbon receptor ligands: implications for toxicity and xenobiotic detoxification. *Expert Opin Drug Metab Toxicol*. 2013;9(2):141–152. doi:10.1517/17425255.2013.738194
50. Nebert DW, Dalton TP, Okey AB, Gonzalez FJ. Role of aryl hydrocarbon receptor-mediated induction of the CYP1 enzymes in environmental toxicity and cancer. *J Biol Chem*. 2004;279(23):23847–23850. doi:10.1074/jbc.R400004200
51. Tsay A, Wang JC. The role of PIK3R1 in metabolic function and insulin sensitivity. *Int J Mol Sci*. 2023;24(16):12665. doi:10.3390/ijms241612665

52. Li H, Lin R, Zhang Y, et al. N6-methyladenosine-modified circPLPP4 sustains cisplatin resistance in ovarian cancer cells via PIK3R1 upregulation. *Mol Cancer*. 2024;23(1):5. doi:10.1186/s12943-023-01917-5
53. Mohamed R, Jayakumar C, Ranganathan PV, Ganapathy V, Ramesh G. Kidney proximal tubular epithelial-specific overexpression of netrin-1 suppresses inflammation and albuminuria through suppression of COX-2-mediated PGE2 production in streptozotocin-induced diabetic mice. *Am J Pathol*. 2012;181(6):1991–2002. doi:10.1016/j.ajpath.2012.08.014
54. Wang Q, Morris RJ, Bode AM, Zhang T. Prostaglandin pathways: opportunities for cancer prevention and therapy. *Cancer Res*. 2022;82(6):949–965. doi:10.1158/0008-5472.CAN-21-2297
55. Luo LP, Suo P, Ren LL, Liu HJ, Zhang Y, Zhao YY. Shengkang injection and its three anthraquinones ameliorates renal fibrosis by simultaneous targeting I $\kappa$ B/NF- $\kappa$ B and Keap1/Nrf2 signaling pathways. *Front Pharmacol*. 2021;12:800522. doi:10.3389/fphar.2021.800522
56. Zhou Q, Tian W, Jiang Z, et al. A positive feedback loop of AKR1C3-mediated activation of NF- $\kappa$ B and STAT3 facilitates proliferation and metastasis in hepatocellular carcinoma. *Cancer Res*. 2021;81(5):1361–1374. doi:10.1158/0008-5472.CAN-20-2480
57. Henamayee S, Banik K, Sailo BL, et al. Therapeutic emergence of rhein as a potential anticancer drug: a review of its molecular targets and anticancer properties. *Molecules*. 2020;25(10):2278. doi:10.3390/molecules25102278

## Drug Design, Development and Therapy

### Publish your work in this journal

Drug Design, Development and Therapy is an international, peer-reviewed open-access journal that spans the spectrum of drug design and development through to clinical applications. Clinical outcomes, patient safety, and programs for the development and effective, safe, and sustained use of medicines are a feature of the journal, which has also been accepted for indexing on PubMed Central. The manuscript management system is completely online and includes a very quick and fair peer-review system, which is all easy to use. Visit <http://www.dovepress.com/testimonials.php> to read real quotes from published authors.

Submit your manuscript here: <https://www.dovepress.com/drug-design-development-and-therapy-journal>

**Dovepress**  
Taylor & Francis Group